

NOAA Technical Memorandum ERL PMEL-68

WATER PROPERTIES AND CIRCULATION IN SHELIKOF STRAIT, ALASKA DURING 1985

R. K. Reed
J. D. Schumacher

L. S. Incze
College of Ocean and Fishery Sciences
University of Washington
and
Northwest and Alaska Fisheries Center
Seattle, Washington

Pacific Marine Environmental Laboratory
Seattle, Washington
October 1986



**UNITED STATES
DEPARTMENT OF COMMERCE**

**Malcolm Baldrige,
Secretary**

NATIONAL OCEANIC AND
ATMOSPHERIC ADMINISTRATION

Anthony J. Calio,
Administrator

Environmental Research
Laboratories

Vernon E. Derr,
Director

NOTICE

Mention of a commercial company or product does not constitute an endorsement by NOAA Environmental Research Laboratories. Use for publicity or advertising purposes of information from this publication concerning proprietary products or the tests of such products is not authorized.

For sale by the National Technical Information Service, 5285 Port Royal Road
Springfield, VA 22161

CONTENTS

	<u>Page</u>
1. INTRODUCTION.....	1
2. DATA AND METHODS.....	3
3. ESTUARINE-TYPE CIRCULATION.....	5
4. PHYSICAL PROPERTIES.....	9
5. NUTRIENTS.....	22
6. BAROCLINIC FLOW.....	22
7. VOLUME TRANSPORT.....	28
8. DISCUSSION.....	32
9. CONCLUSIONS.....	32
10. ACKNOWLEDGMENTS.....	34
11. REFERENCES.....	35

WATER PROPERTIES AND CIRCULATION IN SHELIKOF STRAIT, ALASKA DURING 1985

R.K. Reed¹
J.D. Schumacher¹
L.S. Incze²

ABSTRACT. Data from cruises in March, July, and October 1985 are used to describe circulation and property distributions, and their changes, in Shelikof Strait. The Alaska Coastal Current flows to the southwest throughout the year, but greatest baroclinic, geostrophic speeds occur in fall when the upper waters are least saline because of a maximum in freshwater discharge. The deep water in the central part of the Strait has its source to the south, and the properties seem to result from vertical mixing of this southern water. Thus Shelikof Strait has an estuarine-like circulation, but the intensity of the northward inflow varies appreciably.

Property distributions showed isolines were nearly always deepest on the right side of the channel (looking downstream); greatest baroclinic speeds were often there also. It is believed that differential Ekman pumping may be important to the development of this structure and its changes, at least in some locations. Volume transport estimates for the upper 150 db varied greatly in space and time, with maximum values $>10^6 \text{ m}^3 \text{ s}^{-1}$. At times the southwest flow bifurcated, with part continuing along the Alaska Peninsula and the rest exiting the main channel to the south.

1. INTRODUCTION

The observations examined here were obtained as part of the Fishery Oceanography Coordinated Investigations (FOCI) of NOAA. This program is a long-term, joint effort by the Pacific Marine Environmental Laboratory and the Northwest and Alaska Fisheries Center of the National Marine Fisheries Service. Its goal is to gain understanding of the influence of biotic and abiotic environments on recruitment of various commercially valuable fish and shellfish stocks. The FOCI work in 1985 was in Shelikof Strait, Alaska (see Fig. 1) where large concentrations of spawning pollock occur during spring (Nelson and Nunnallee, 1986). Dense concentrations of eggs and larvae result, and the larvae are transported southwestward as they develop (Schumacher et al., 1985). Our hypothesis is that survival of larvae and juvenile fish is greatest for those which remain in waters along the Alaska Peninsula, as opposed to being removed from the shelf. This study deals primarily with the

¹ Pacific Marine Environmental Laboratory/NOAA, 7600 Sand Point Way NE, Seattle, WA, 98115

² College of Ocean and Fishery Sciences, University of Washington, Seattle, WA, 98195, and Northwest and Alaska Fisheries Center/NOAA, 7600 Sand Point Way NE, Seattle, WA, 98115

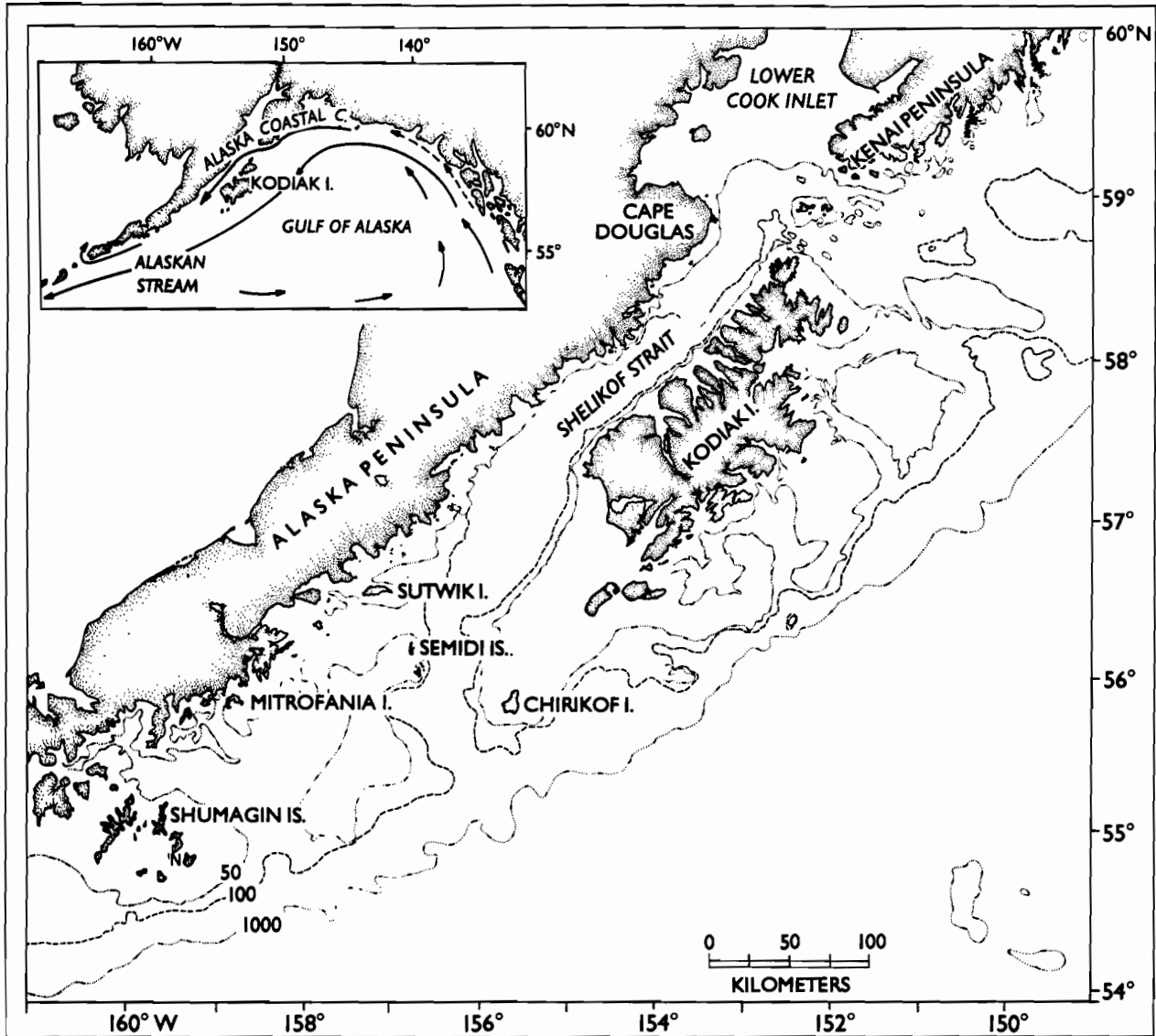


Figure 1.--Location of the study area with place names and the bathymetry (in fathoms; 1 fathom = 1.83 m). The insert indicates the typical upper-ocean circulation.

physical environment as observed during cruises in March, July, and October 1985.

Previous oceanographic observations in Shelikof Strait are quite limited. Two early studies of parts of this region were those of Favorite and Ingraham (1977) and Schumacher et al. (1978). Schumacher and Reed (1980) analyzed temperature-salinity data and current measurements in the northern part of the Strait, and Reed and Schumacher (1986) included some information on the area in their review. Finally, Schumacher and Reed (1986) have examined conditions in the southern Strait and along the Alaska Peninsula. It is now apparent that the upper waters of Shelikof Strait are affected by the Alaska Coastal Current (ACC; Royer, 1981), which enters the Strait after flowing along the Kenai Peninsula. The ACC flows down the Strait; near the Semidi Islands (Fig. 1) the flow sometimes bifurcates, with one branch continuing along the Alaska Peninsula and the other moving seaward (Schumacher and Reed, 1986). Waters in the ACC are characterized by relatively low salinity (Royer, 1981), which usually reaches a minimum in fall as a result of a maximum in freshwater discharge then.

2. DATA AND METHODS

Cruises were conducted aboard the NOAA ship DISCOVERER in March and July 1985 and on the NOAA ship MILLER FREEMAN in October 1985. The CTD (conductivity/temperature/depth) casts made during these periods are shown in Fig. 2. The same numbered grid was used throughout, but every station was not occupied on each cruise. Stations with the same number, however, were at essentially the same site. The grid was not always occupied in the same order, but the general progression can be inferred from the dates given in Tables 3-5 below. It should be noted that the bathymetry shown on the figures is not highly reliable everywhere; major troughs and shoals, however, are essentially as depicted. In addition to measuring physical properties, sampling for nutrients, chlorophyll, and zooplankton was conducted. Current meter moorings were also deployed at ten sites (along the lines between stations 152-158, 147-151, 55-61, and at M10; see Fig. 2). Except for nutrients, analysis of these data is not complete, and they will not be used in detail here.

CTD casts were made with a Grundy model 9040 system (March and July) and with a Seabird model 5SBE-9-02 system (October). The Grundy system sampled five times per second for values of temperature, conductivity and pressure; the Seabird system sampled 24 times per second. Data were recorded only during the downcast using a lowering rate of about 30 m/min. Bottle samples were taken at most stations to provide temperature and salinity calibration. Data from monotonically increasing depth were "despiked" to eliminate excessive values and were averaged over 1-m intervals to obtain temperature and salinity from which density and geopotential anomaly were computed.

Water samples were collected for nutrient analyses using 10-l Niskin bottles deployed on the CTD-rosette sampler. Approximately 200 ml of water were transferred from each sample to seasoned 250-ml polyethylene bottles and frozen until analysis ashore. Samples generally were obtained from 0, 5, 10, 20, 30, 50, 75 and 100 m depth, and then at 50-m intervals until 10-20 m off the bottom. During later cruises, additional samples were taken below 100 m

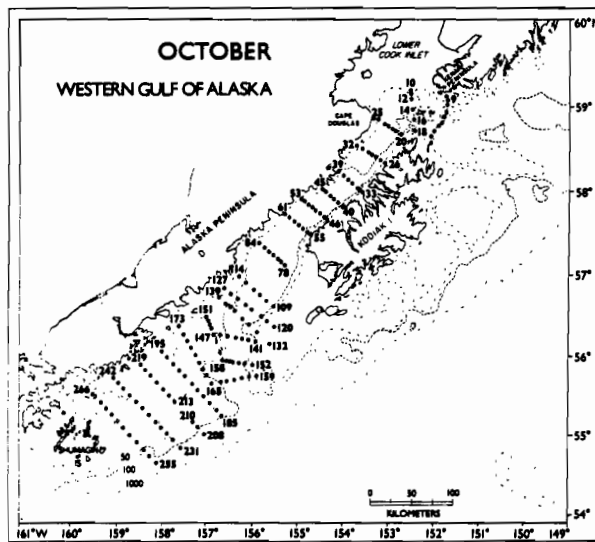
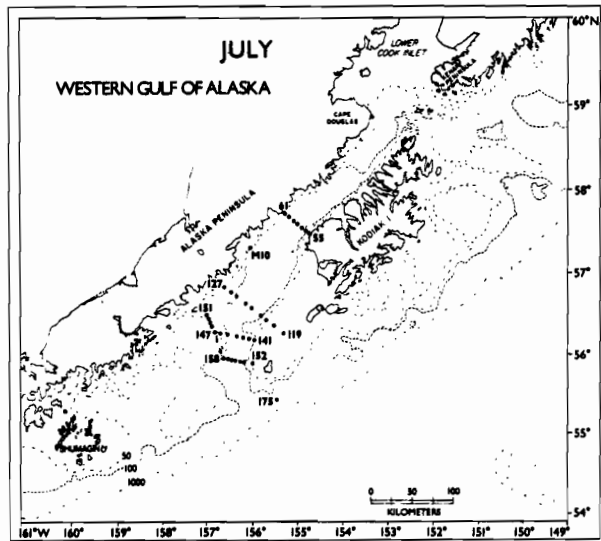
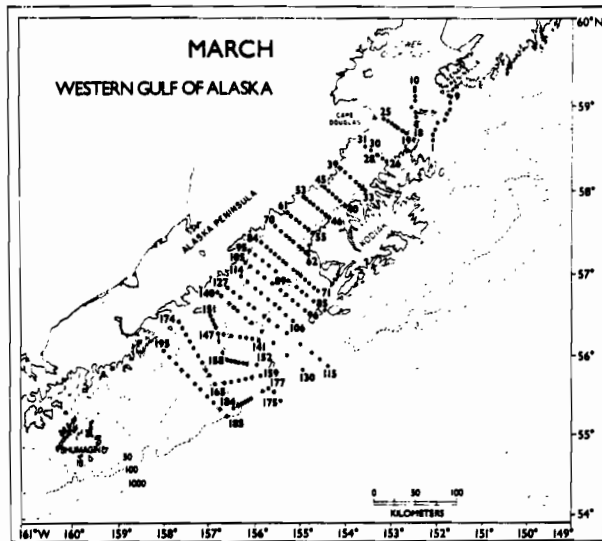


Figure 2.--Location of CTD stations during 12-28 March 1985, 25-28 July 1985, and 9-25 October 1985.

(generally at 25-m intervals) at selected stations. Analyses were performed on a Technicon Autoanalyzer II following methods of Whitley et al. (1981), providing measurements of NO_3 , NO_2 , NH_3 , PO_4 , and SiO_4 . Random measurement error is estimated as <2% of the concentration.

3. ESTUARINE-TYPE CIRCULATION

Upon initial examination of the CTD data, a major question soon became apparent. What is the source of the deep and bottom waters in Shelikof Strait? Is it simply the deeper portion of the entering ACC water, or is it northward intrusions of slope water from the southern end of the Strait as suggested by Schumacher et al. (1978)? That is, does the system have a circulation pattern similar to an estuary? Resolving this question seemed crucial to gaining understanding of the changes in properties and to establishing an appropriate reference level for computing baroclinic flow.

Fig. 3 shows vertical sections of sigma-t density during the three cruises from the southern end of the Strait (left side) to the northern end (right side) using stations approximately in mid-channel. It is immediately apparent that the entering ACC water (station 9, or other stations on this line) was not dense enough in either March or October to be the source of water below about 150 m. Furthermore, in March the isopycnal slopes below about 150 m are strongly suggestive of penetration of deep water from the south or an estuarine-type circulation (cf. Bretschneider et al., 1985). (Because of the width of the Strait, we expect flows to be quasi-geostrophic, but the section shows that a suitable pressure gradient existed for initiating inflows.) The deep slopes in July and October were less extreme, which, coupled with other information to be presented, suggests that the intensity of the inflow varies. Perhaps an even stronger argument for an estuarine-like system is the distribution of nitrate (Fig. 24 below); the entering ACC waters do not have concentrations $>15 \mu\text{g-at}/\ell$, but the deep waters have values $\sim 30 \mu\text{g-at}/\ell$ and must have their source in the deep waters to the south.

It seemed possible that some type of water mass analysis might provide further insight on the formation and circulation of the deeper waters. Fig. 4 presents temperature-salinity plots at station 153 (near the southern entrance to the Strait) and at Station 61 (off the Alaska Peninsula near 58°N) for March, July, and October. The plots for July and October suggest that the bottom water at station 61 could have been formed by mixing of the temperature minimum, temperature maximum, and bottom waters of station 153. In March, however, the bottom water at station 61 was too warm to result from this three-point mixing unless perhaps the bottom water at station 153 had cooled recently and the properties at station 61 resulted from mixing of previous water types. Results from thermistors near the bottom at current meters along the section between stations 152 and 158 indicate that the February temperature was about 5.8°C with rapid cooling in March, which supports the concept advanced.

Mixing triangles for the "water types" at station 153 were constructed, and the percentage of these types at various stations at the bottom were determined for the July and October data (Table 1). In July the percentage of temperature minimum water showed some increase with distance from the source. This would be expected as it is farthest removed vertically from the

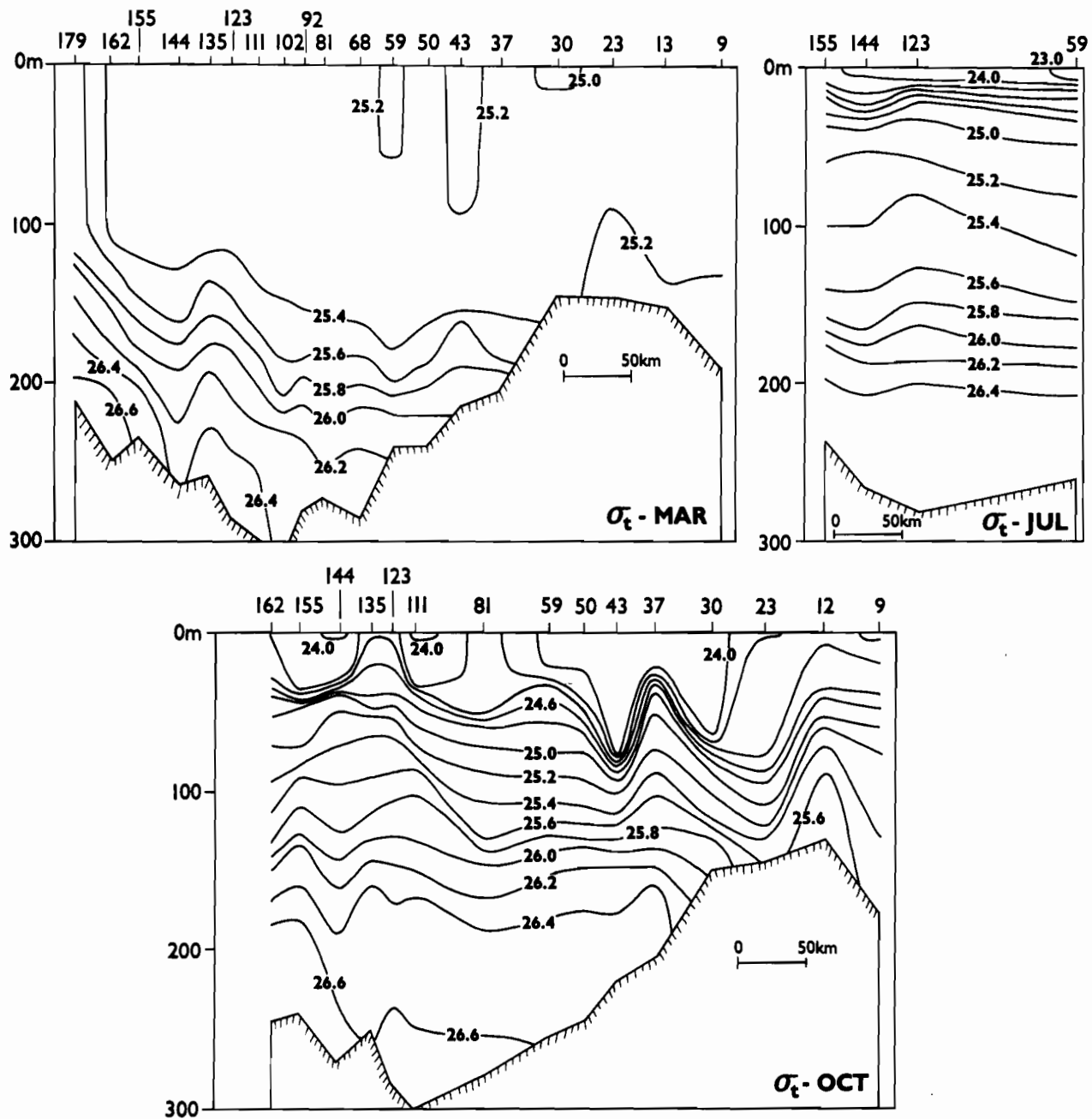


Figure 3.--Vertical sections of sigma-t density along the main channel in Shelikof Strait during March, July, and October 1985.

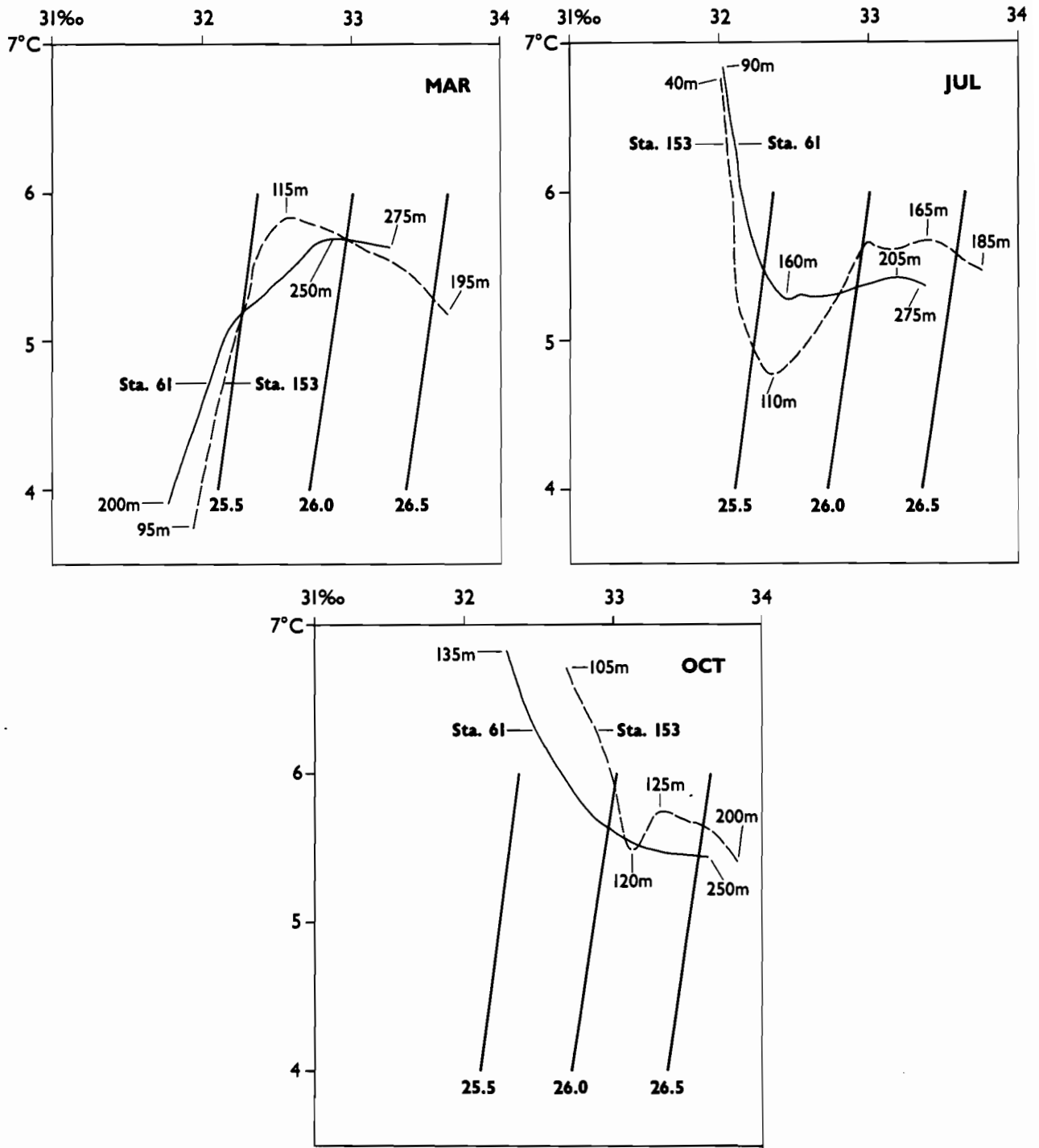


Figure 4.--Temperature-salinity diagrams at stations 153 and 61 for March, July, and October 1985.

Table 1.--Percentages of water types at various stations at the bottom in July and October 1985. Water types are based on temperature-salinity characteristics for station 153 at the temperature minimum, temperature maximum, and the bottom.

Station	July			October		
	% temp. min.	% temp. max.	% bottom	% temp. min.	% temp. max.	% bottom
144	0	55	45	10	0	90
124	20	30	50	30	0	70
122	15	40	45	25	0	75
61	20	25	55	25	5	70
59	20	5	75	15	15	70
57	20	35	45	20	5	75

Table 2.--Temperature ($^{\circ}\text{C}$) and salinity (‰) at the temperature minimum, temperature maximum, and the bottom at stations 153 and 61 as observed in March, July, and October 1985.

Month	Sta. 153			Sta. 61		
	T, S _{min.}	T, S _{max.}	T, S _{bottom}	T, S _{min.}	T, S _{max.}	T, S _{bottom}
March	surface	5.84, 32.56	5.19, 33.65	surface	5.70, 32.85	5.64, 33.26
July	4.78, 32.35	5.67, 33.40	5.47, 33.76	5.28, 32.46	5.42, 33.20	5.38, 33.38
October	5.48, 33.13	5.75, 33.34	5.41, 33.82	none	surface	5.44, 33.62

bottom. Curiously though there was little influence of the temperature maximum water in October. Perhaps this also resulted from a temporal change in water properties and the fact that mixing is not instantaneous. Table 2 shows the variability in water properties at station 153 and station 61. Large changes apparently occur at both stations. The bottom waters were more homogeneous in the Strait, however, in July and October than in March.

Although baroclinic flow in Shelikof Strait may not be entirely geostrophic, the results obtained seem reasonable and are informative. We thus turn to the problem of a reference level for the computations. Initially, volume transport in March was computed from the deepest common depth between adjacent stations. This resulted in over twenty-fold variations between nearby sections and some implausibly large values ($>2 \times 10^6 \text{ m}^3/\text{sec}$). (The July and October results were less sensitive to choice of a reference level because most of the vertical shear in geopotential anomaly difference occurred farther up in the water column than in March.) Since we are convinced that the source waters for deep water in Shelikof Strait are to the south and that an estuarine-type circulation exists, at least at times, an intermediate reference level should be used. We do not imply that a single "level of no motion," invariant over space and time, actually exists. An intermediate level yields much more plausible results than computations referred to the bottom, however. We have chosen 150 db, and it is used throughout. Limited support for this choice is available from Figs. 3 and 24 and from the August 1984-July 1985 current measurements at three moorings on the section between stations 152 and 158. Meters on the three moorings at 185, 205, and 165 m all showed weak northward flow, with weak southward flow above at levels of 105, 120, and 120 m.

4. PHYSICAL PROPERTIES

Surface salinity distributions are a useful index of the path of the ACC (Schumacher and Reed, 1980; Royer, 1981) and are shown in Fig. 5. In March the inflowing ACC off the Kenai Peninsula had salinity less than 31.75‰ ; these values were generally continuous throughout the system, except at the lower end of the Strait where salinity was higher. The lowest values occurred off Cape Douglas, presumably the result of intrusions from Lower Cook Inlet. In July the lowest-salinity water (about 1‰ less than in March) was generally quite close to the Alaska Peninsula. October salinities were similar to those in July. In the northern Strait, there were small regions of both low and high salinity. Compared with fall 1977 (Schumacher and Reed, 1986), salinity was higher in fall 1985. This is consistent with results which show fall 1977 as having relatively low salinity in the ACC off the Kenai Peninsula (Xiong and Royer, 1984).

We also mapped temperature on the sigma-t surface of 26.2 (typically 150-250-m depths), and the results are presented in Fig. 6. In all three months the largest gradients were at the southern end of the Strait, and temperatures to the north varied little more than 0.1°C . This pattern suggests that deep waters attain their properties rather abruptly and not through uniform lateral mixing. We suspect that vertical mixing, aided by tidal currents, is the mechanism. The fact that bottom water properties to the north seem to have components of southern temperature minimum and maximum waters (Table 1) also supports the existence of vertical mixing.

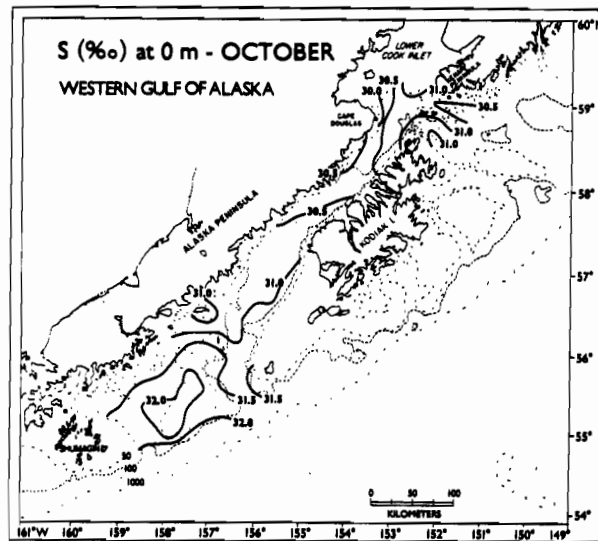
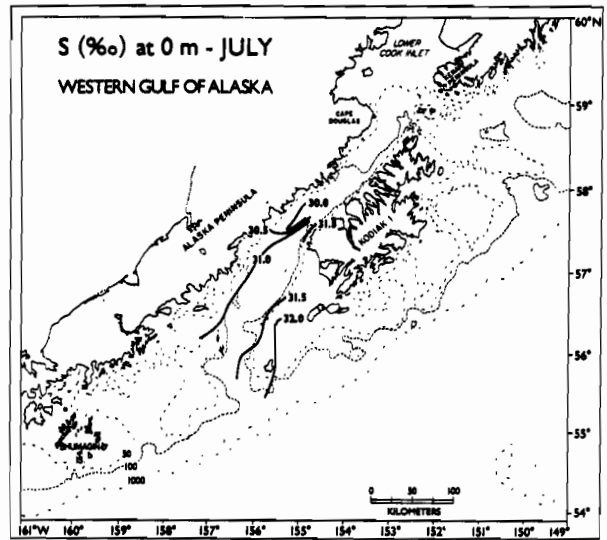
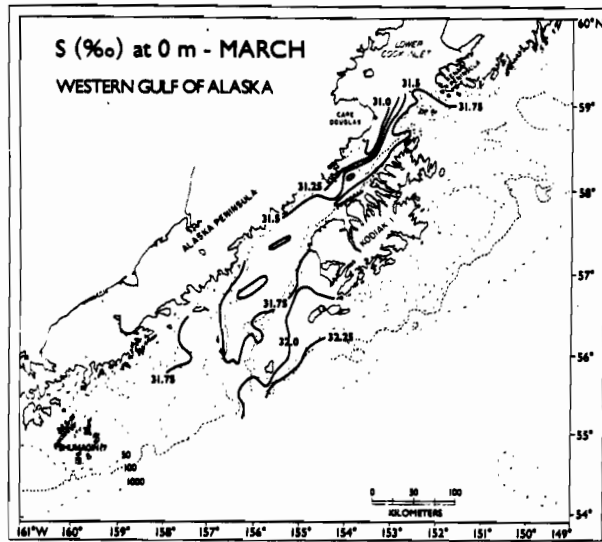


Figure 5.--Surface salinity (‰) during March, July, and October 1985.

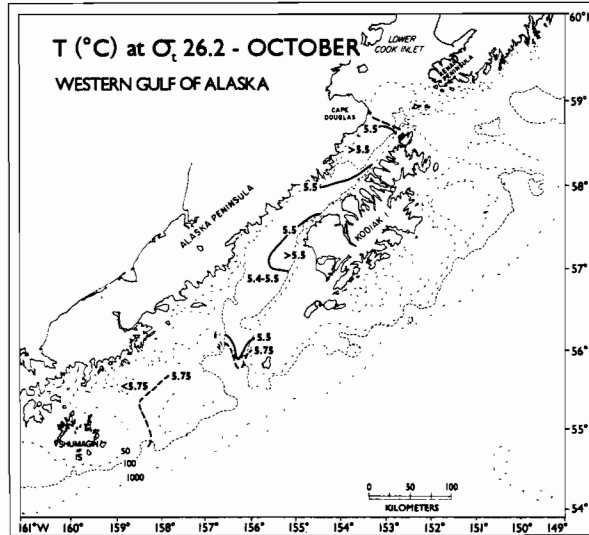
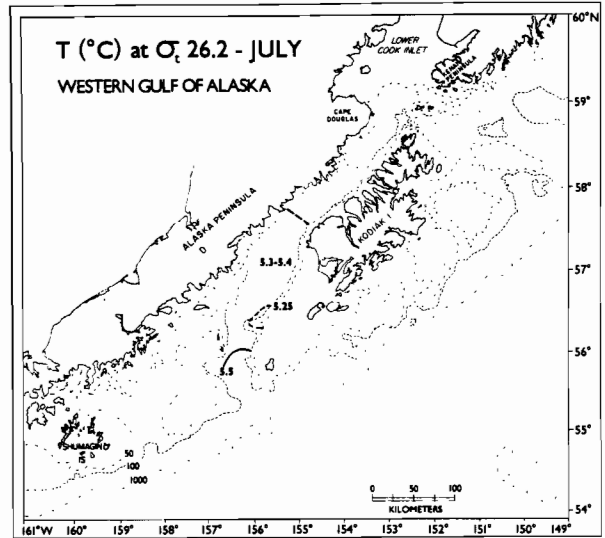
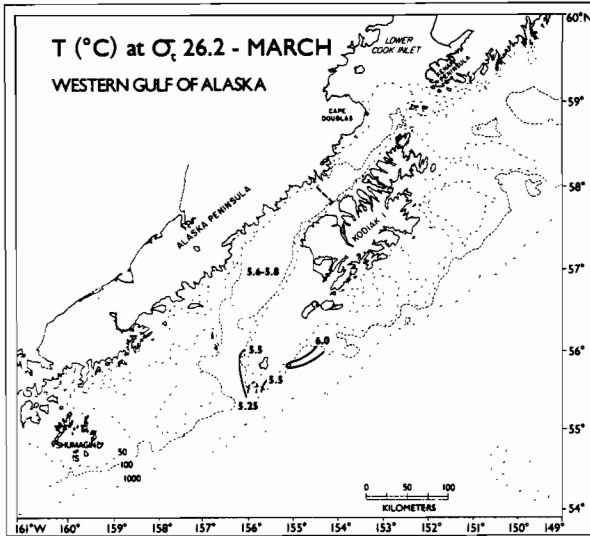


Figure 6.--Temperature (°C) at the sigma-t density of 26.2 during March, July, and October 1985. Dashed lines indicate the northern limit of data coverage.

March vertical sections. Vertical sections of temperature, salinity, sigma-t density, and geostrophic flow are presented for seven across-channel lines for March in Figs. 7-13. (Note that flow is not shown below the reference level chosen, 150 db, or the deepest common level between adjacent stations in lesser depths.) The orientation of the sections is as follows: those which are essentially north-south (stations 1-9 and 147-151) are shown with north on the right; the others, which are more nearly east-west, are shown with west (Alaska Peninsula side) to the left. Also, flow to the west or south is shown unhatched; those in opposite directions are hatched. In Fig. 7 steeply sloped isolines of all properties occurred between stations 6 and 9, and the flow was consistently westward in agreement with these features. To the south, the isolines display a domed feature and then reverse. Fig. 8 shows steeply sloped isolines near the Alaska Peninsula; computed speeds were in excess of 25 cm s^{-1} , with a reversal near Kodiak Island. Fig. 9 shows maximum southwest flow near Kodiak Island, however, rather than near the Alaska Peninsula. Note also that high speeds extend much deeper in the water column than in Fig. 8. Figs. 10 and 11 display similar features. The steepest slopes and highest speeds were near Kodiak Island; there were weak reversals, but speeds were considerably smaller than on the previous two sections. Fig. 12 shows fairly steep slopes everywhere except between station 152 and 153. The strongest southward flow was in mid-channel. Fig. 13 crosses the relatively shallow shelf region near the Alaska Peninsula at about 157°W . There were virtually no slopes, and the baroclinic flow was insignificant.

July vertical sections. Figure 14 shows cooler, more saline deep water than was present here in March; the isolines were also less steeply sloped, and produced weaker flow below 50 m, than in winter. Fig. 15 indicates strong flow ($>35 \text{ cm/sec}$) near the Alaska Peninsula, with reversals elsewhere in the channel. Fig. 16 shows some reversals in isoline slopes near the surface which were opposite to the slopes below. Flow was generally southward though, and the highest speeds occurred on the right side looking down-channel. Unlike in March, Fig. 17 indicates westward flow in the shallow channel near the Alaska Peninsula.

October vertical sections. Fig. 18 shows slopes similar to those in March. Near-surface waters were about 1‰ fresher, but near-bottom waters were more saline than in March, in agreement with previous findings for the ACC (Schumacher and Reed, 1980). In October flow was westward across the northern side of the entrance but was eastward to the south. Fig. 19 indicates fairly strong southwest flow split by northeast flow near the center of the channel. Fig. 20 shows steeply sloped isolines, with strong southwest flow, all across the channel. Maximum speeds were $>45 \text{ cm s}^{-1}$. Fig. 21 indicates complex patterns with flow reversals. Near the southern end of the channel (Fig. 22) even more complexity was present; southward flow occurred near the center of the channel, but there was an appreciable northward flow near the surface on the right side looking downstream. The section between stations 147 and 151 (Fig. 23) shows westward flow along the Alaska Peninsula, with a weak reversal near the coast.

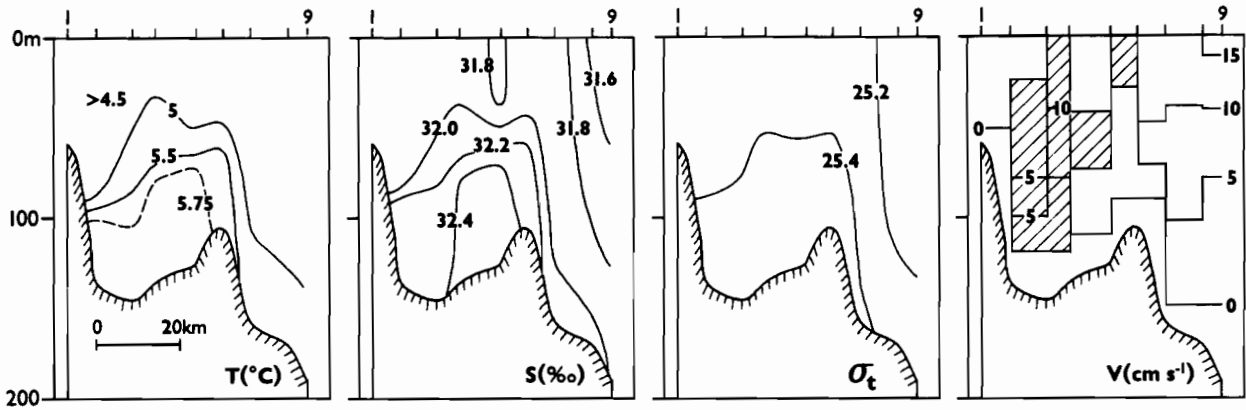


Figure 7.--Vertical sections of temperature ($^{\circ}\text{C}$), salinity (‰), sigma-t density, and geostrophic flow (cm s^{-1}) for stations 1-9, 12-13 March 1985.

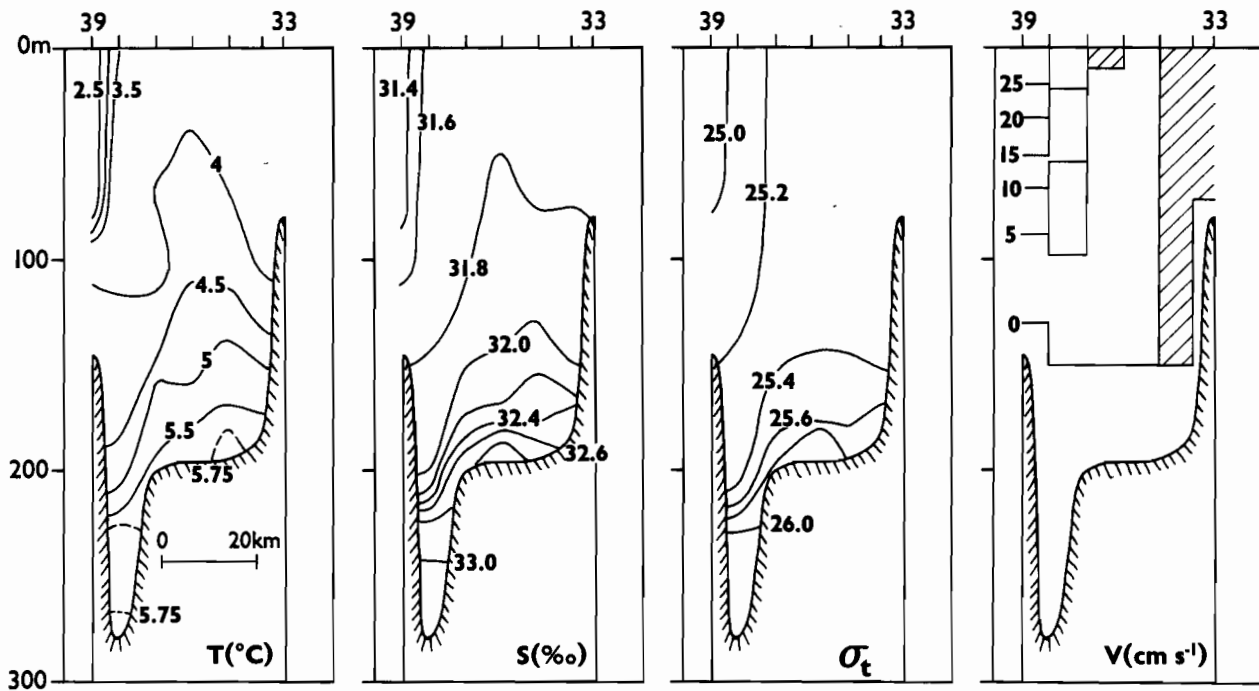


Figure 8.--Vertical sections of temperature ($^{\circ}\text{C}$), salinity (‰), sigma-t density, and geostrophic flow (cm s^{-1}) for stations 33-39, 14-15 March 1985.

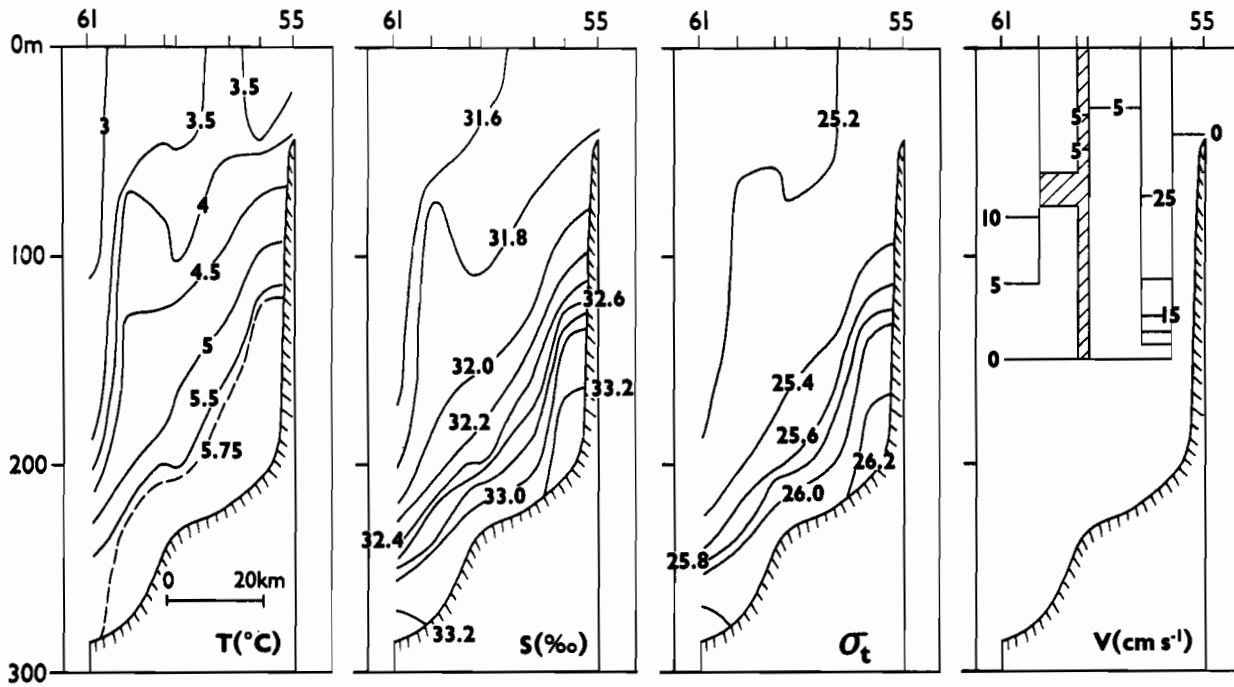


Figure 9.--Vertical sections of temperature ($^{\circ}\text{C}$), salinity (‰), sigma-t density, and geostrophic flow (cm s^{-1}) for stations 55-61, 16 March 1985.

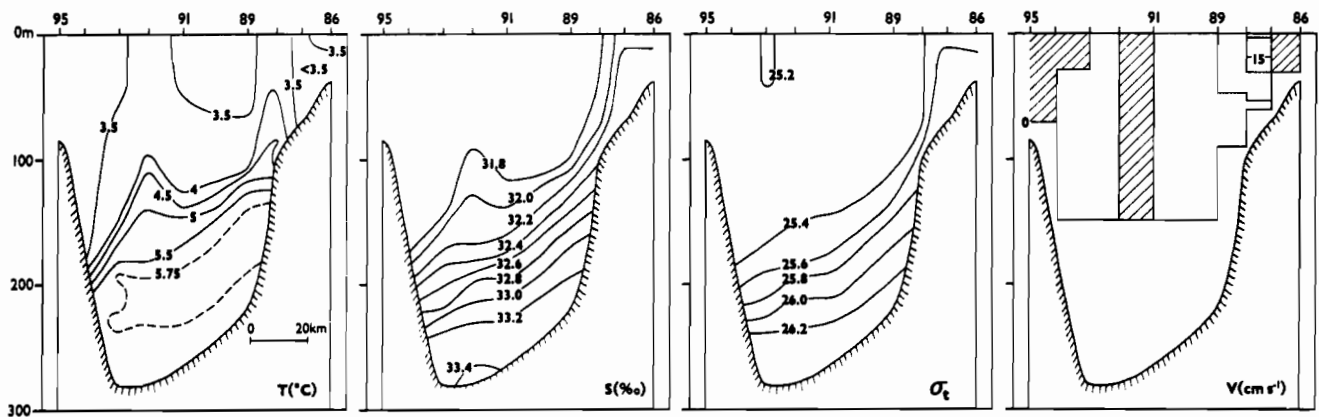


Figure 10.--Vertical sections of temperature ($^{\circ}\text{C}$), salinity (‰), sigma-t density, and geostrophic flow (cm s^{-1}) for stations 86-95, 19-20 March 1985.

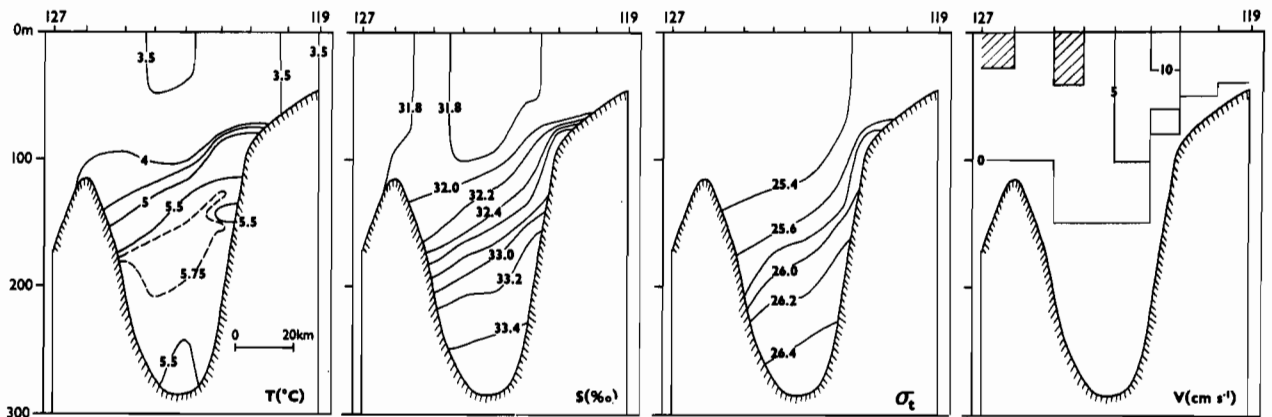


Figure 11.--Vertical sections of temperature ($^{\circ}\text{C}$), salinity (‰), sigma-t density, and geostrophic flow (cm s^{-1}) for stations 119-127, 22 March 1985.

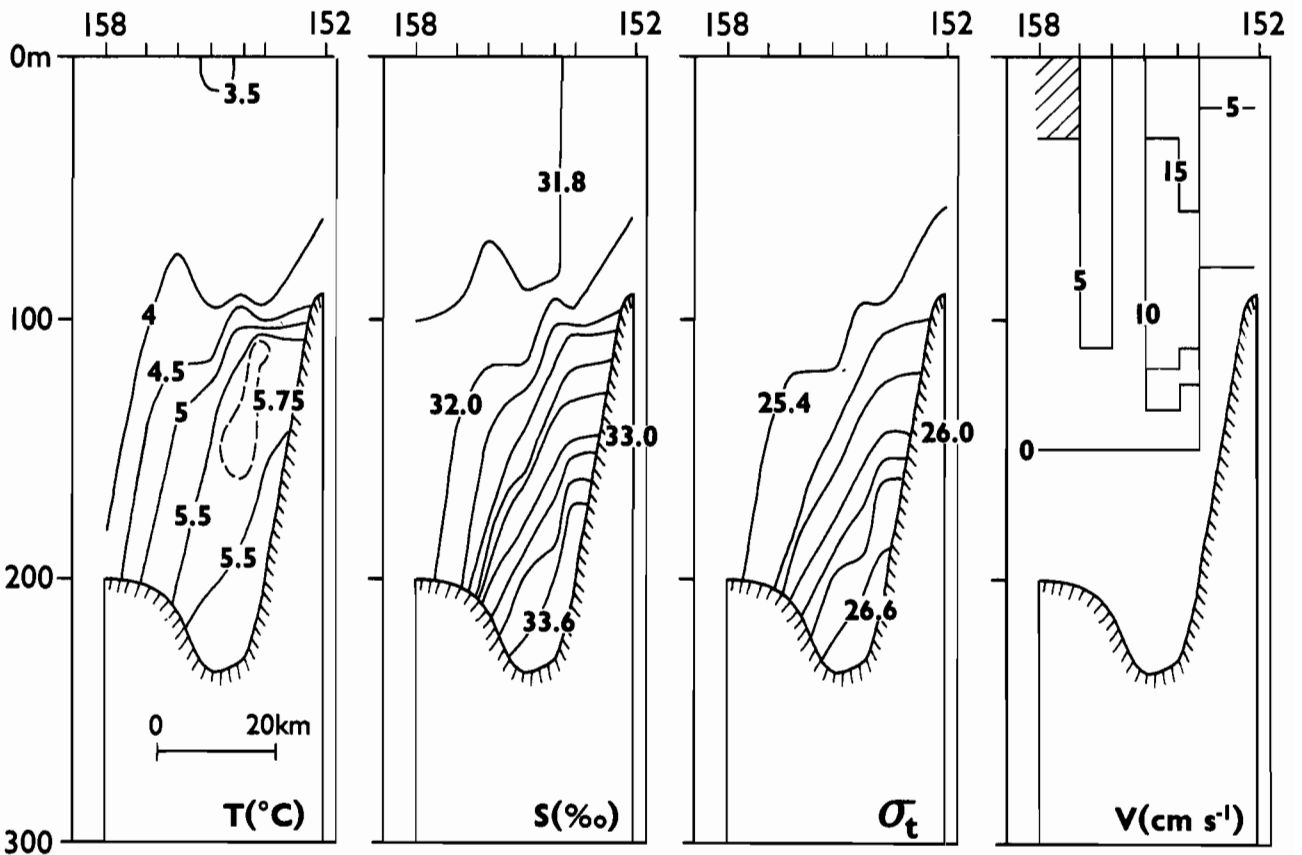


Figure 12.--Vertical sections of temperature ($^{\circ}\text{C}$), salinity (‰), sigma-t density, and geostrophic flow (cm s^{-1}), for stations 152-158, 25 March 1985.

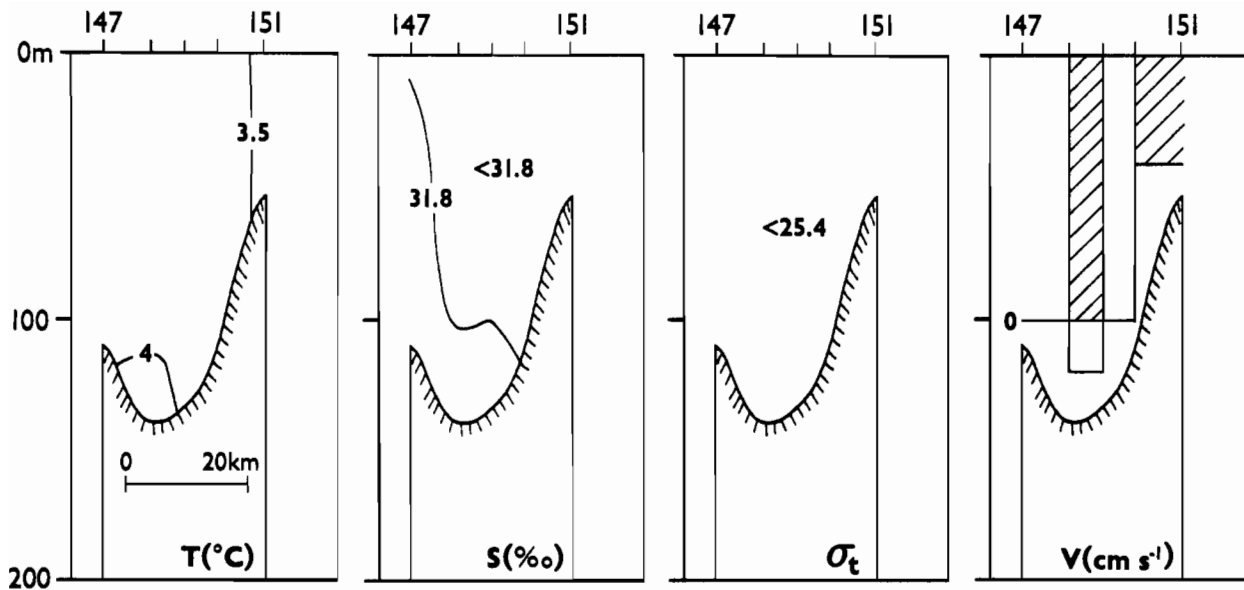


Figure 13.--Vertical sections of temperature ($^{\circ}\text{C}$), salinity (‰), sigma-t density, and geostrophic flow (cm s^{-1}) for stations 147-151, 26 March 1985.

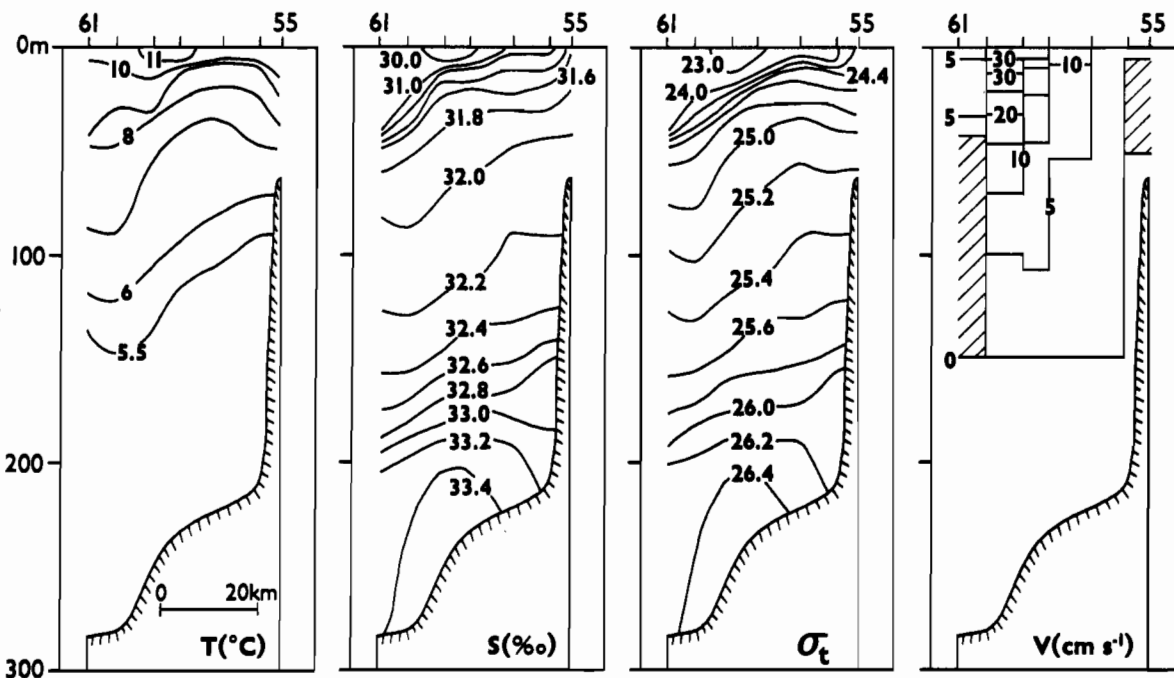


Figure 14.--Vertical sections of temperature ($^{\circ}\text{C}$), salinity (‰), sigma-t density, and geostrophic flow (cm s^{-1}) for stations 55-61, 27-28 July 1985.

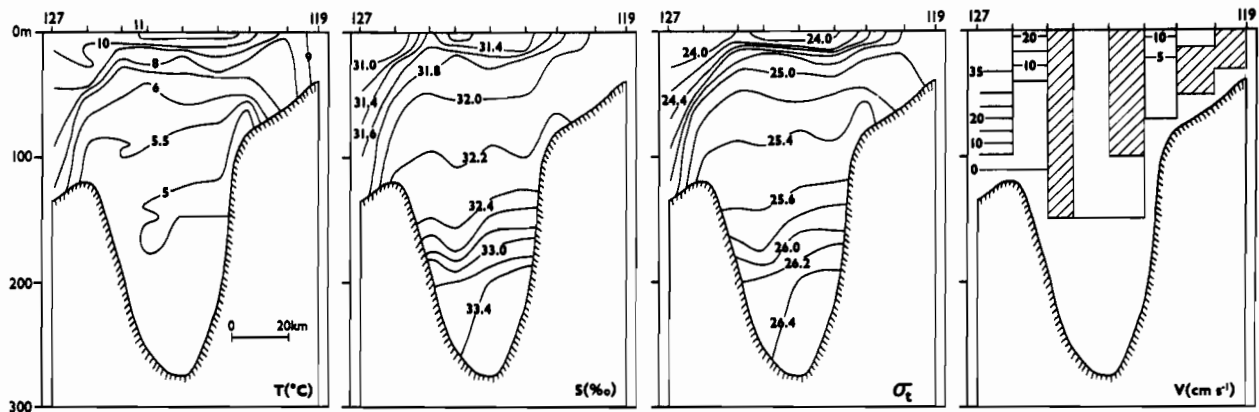


Figure 15.--Vertical sections of temperature ($^{\circ}\text{C}$), salinity (‰), sigma-t density, and geostrophic flow (cm s^{-1}) for stations 119-127, 27 July 1985.

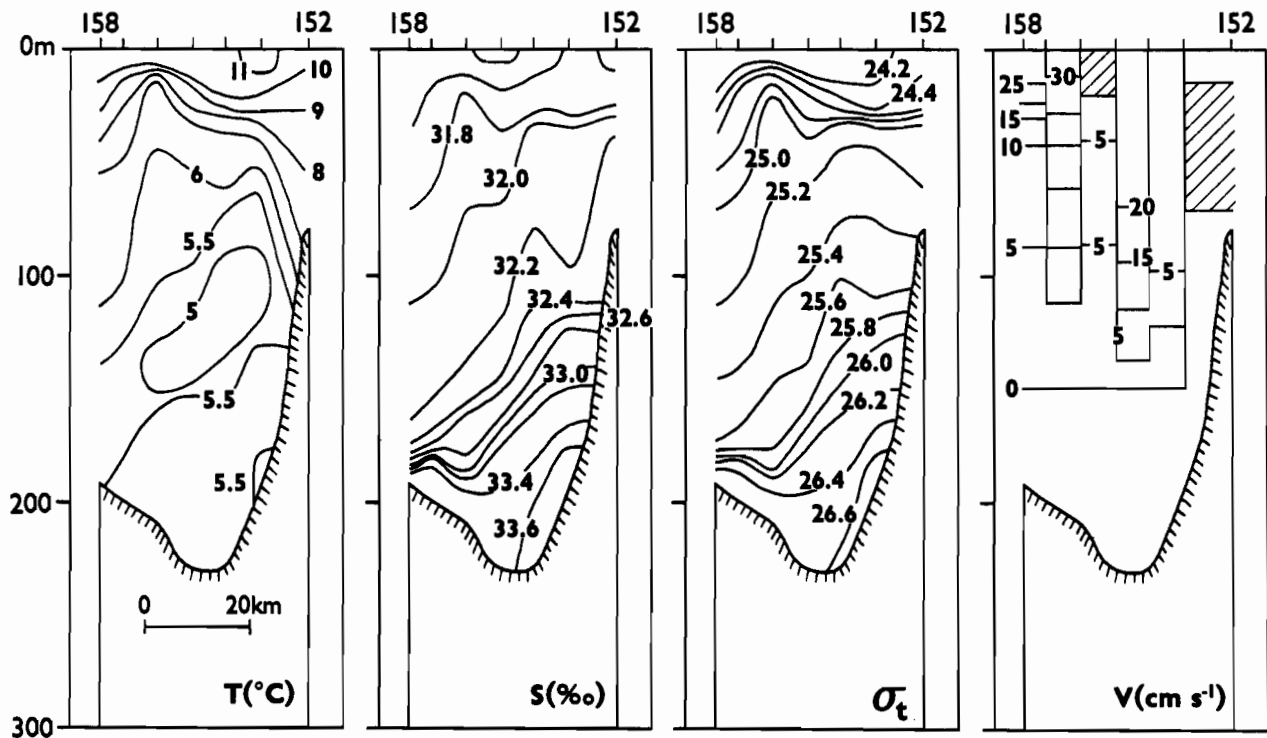


Figure 16.--Vertical sections of temperature ($^{\circ}\text{C}$), salinity (‰), sigma-t density, and geostrophic flow (cm s^{-1}) for stations 152-158, 25-26 July 1985.

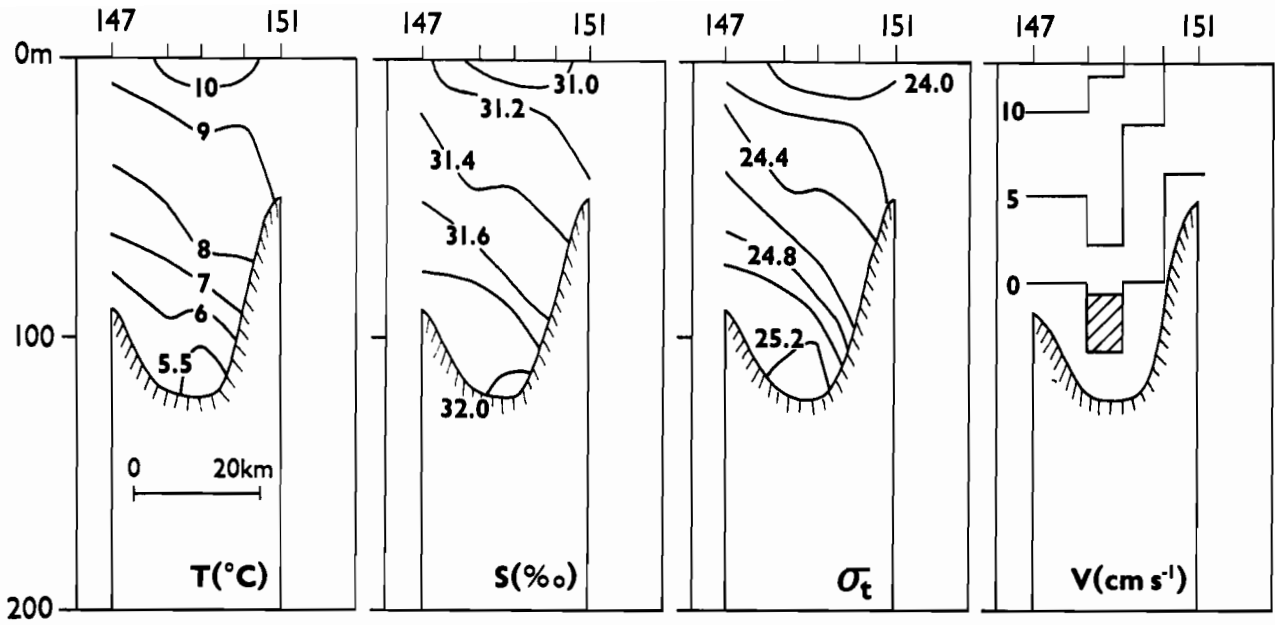


Figure 17.--Vertical sections of temperature ($^{\circ}\text{C}$), salinity (‰), sigma-t density, and geostrophic flow (cm s^{-1}) for stations 147-151, 26 July 1985.

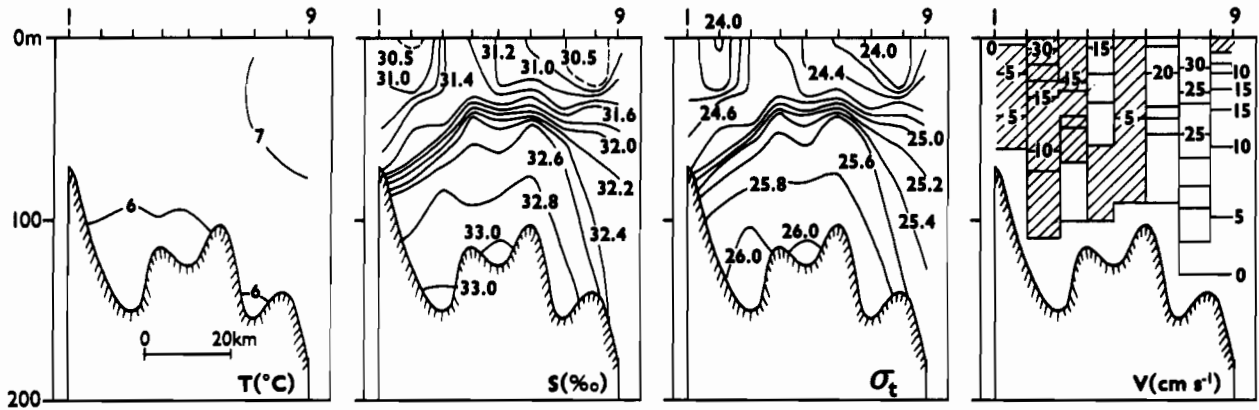


Figure 18.--Vertical sections of temperature ($^{\circ}\text{C}$), salinity (‰), sigma-t density, and geostrophic flow (cm s^{-1}) for stations 1-9, 24-25 October 1985.

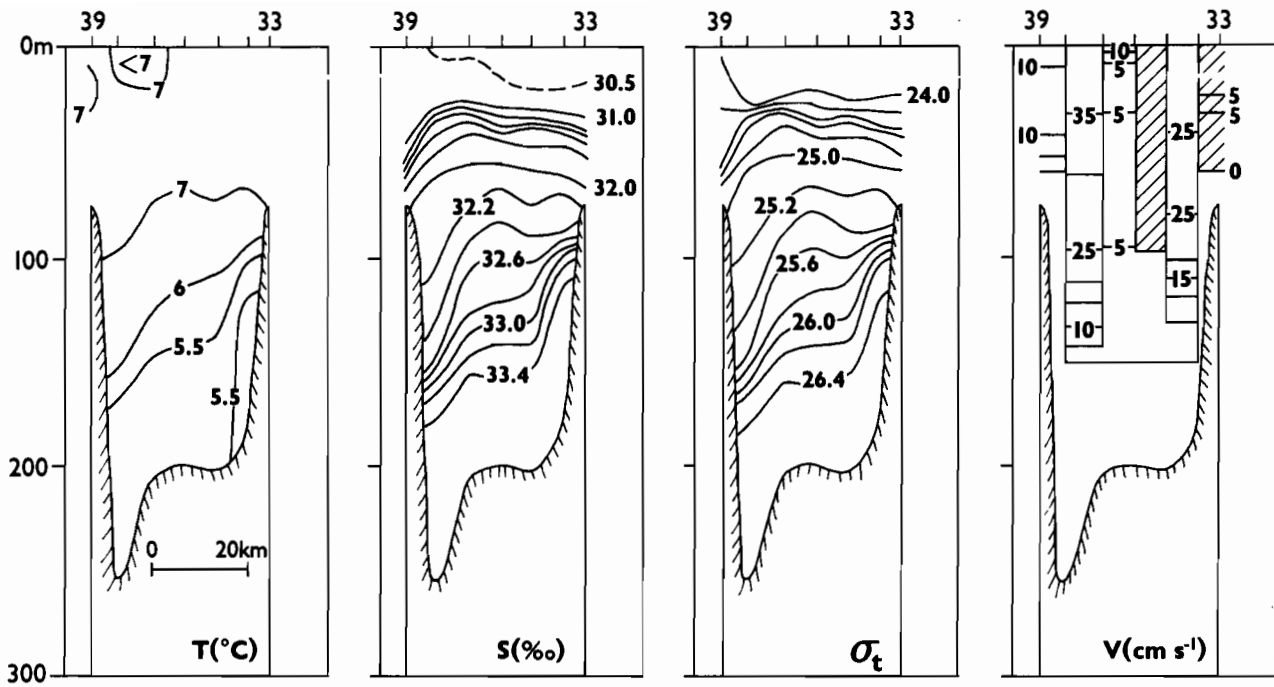


Figure 19.--Vertical sections of temperature (°C), salinity (‰), sigma-t density, and geostrophic flow (cm s⁻¹) for stations 33-39, 22 October 1985.

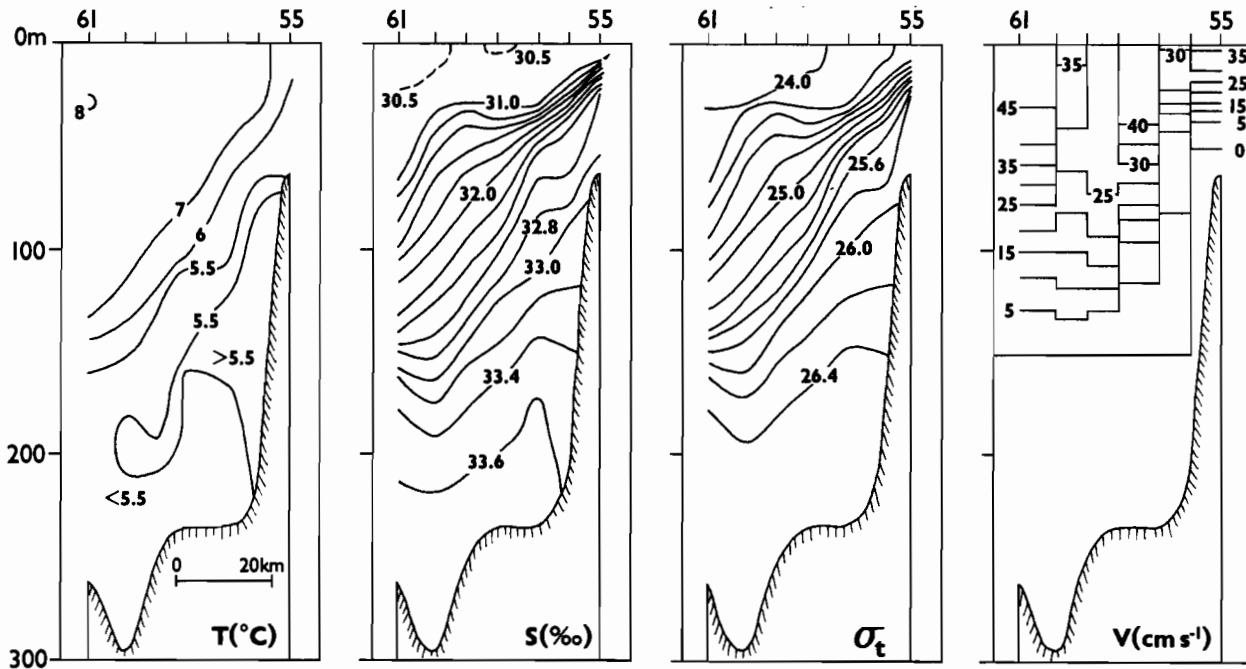


Figure 20.--Vertical sections of temperature (°C), salinity (‰), sigma-t density, and geostrophic flow (cm s⁻¹) for stations 55-61, 21 October 1985.

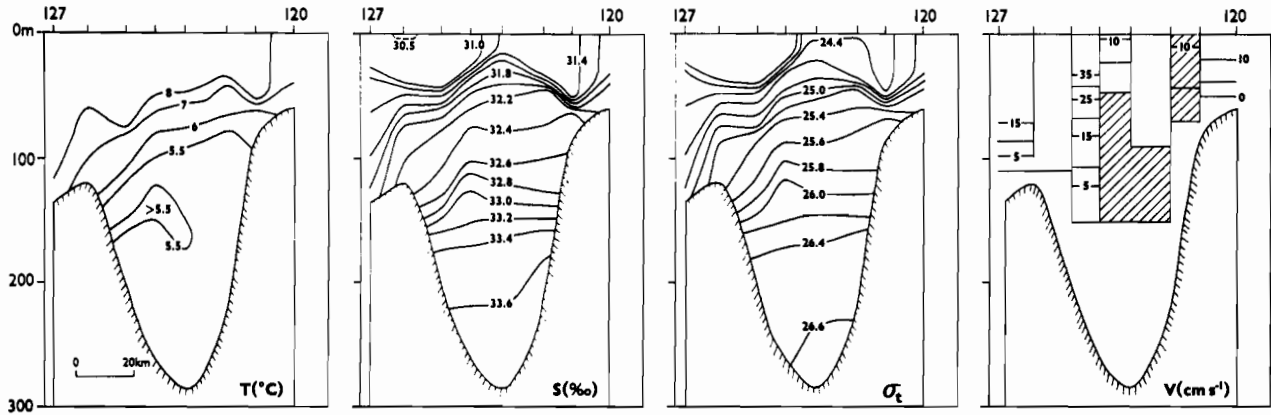


Figure 21.--Vertical sections of temperature ($^{\circ}\text{C}$), salinity (‰), sigma-t density, and geostrophic flow (cm s^{-1}) for stations 120-127, 17 October 1985.

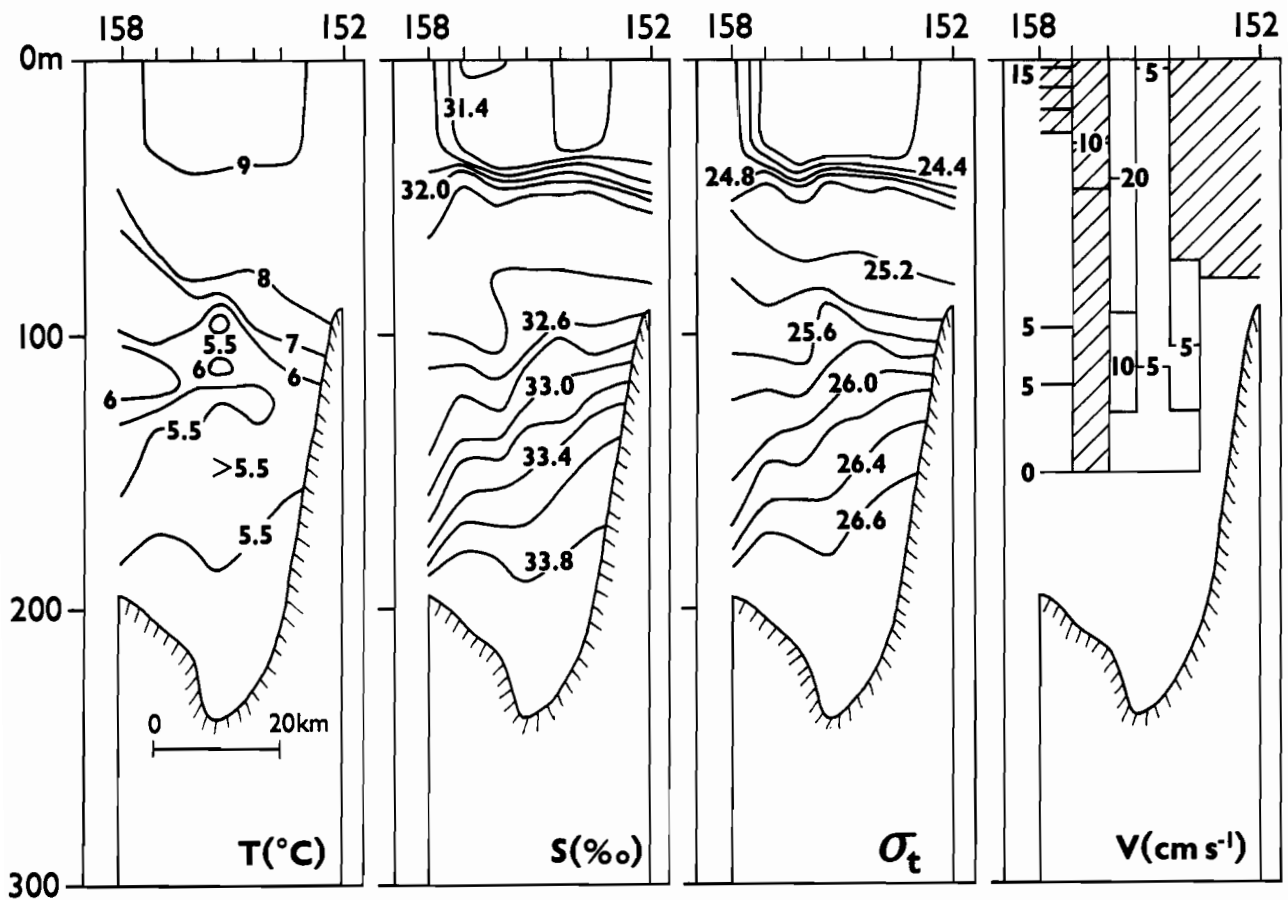


Figure 22.--Vertical sections of temperature ($^{\circ}\text{C}$), salinity (‰), sigma-t density, and geostrophic flow (cm s^{-1}) for stations 152-158, 9 October 1985.

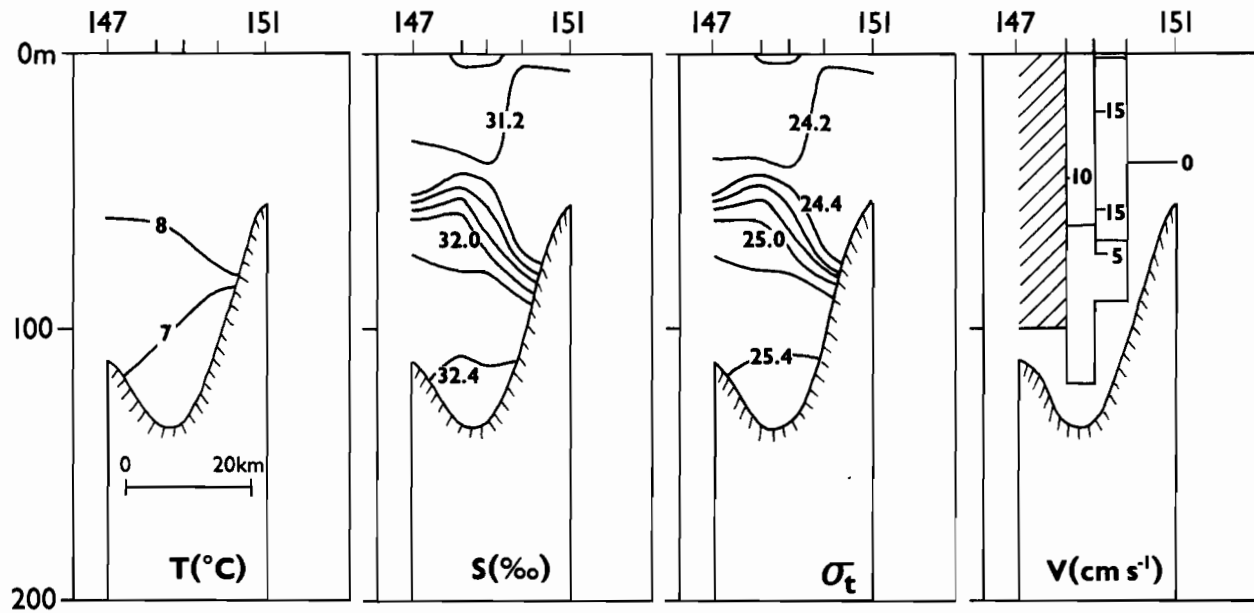


Figure 23.--Vertical sections of temperature (°C), salinity (‰), sigma-t density, and geostrophic flow (cm s⁻¹) for stations 147-151, 11 October 1985.

5. NUTRIENTS

Nitrate and silicate showed the strongest vertical and horizontal gradients of the nutrients examined and were useful indicators of the general circulation. The nitrate data are presented here in Figs. 24-28. Figure 24 shows increased nutrient levels at the southern end of the Strait at all depths during spring and summer. October data show a reversed gradient in the upper water column. NO_3 isopleths suggest that this resulted from greater vertical mixing in the Strait (e.g., station 22) compared to the southern section of the sea valley. Nutrient samples were not obtained as far seaward during October, but data for the deep water indicate the same seaward increase in NO_3 concentration observed during spring and summer. Nutrient data from all three cruises indicate that the deepest water originates from the south, since it is richer in NO_3 than any water north of station 58. In general, NO_3 concentration (Figs. 25-28) was lowest and lower levels extended deepest into the water column near the Alaska Peninsula, in concert with fresher water and deeper upper mixed layers. The seasonal decline of nitrate in surface waters is evident in the change from March to July, with levels being partially restored by October.

6. BAROCLINIC FLOW

Figure 29 presents the geopotential topography at the sea surface referred to 150 db for March, July, and October. In March the ACC entered the passage off the Kenai Peninsula and flowed southwest. The baroclinic circulation in March was relatively weak, except for a region of fairly intense flow near the southern end of the Strait. In July flow near Kodiak Island was stronger than in March. October had by far the most intense baroclinic circulation of the three periods. ACC waters entered the passage off the Kenai Peninsula, but there appeared to be outflow to the south as noted previously in fall (Schumacher and Reed, 1980). The flow had intensified appreciably in the vicinity of Kodiak Island. The isolines suggest considerable meandering, and the current appeared to split off the southern end of Kodiak Island but rejoined farther to the south. At the southern end of the Strait, there was northward inflow on one side and southward outflow at the other. A significant portion of the flow continued westward along the Alaska Peninsula, and this branch appeared to intensify near the western limit of these data. Although the 0/150-db topography did not indicate northward inflow into the region east of the Shumagin Islands, the transport computations below did. It should be stressed that we have been discussing only the baroclinic, geostrophic component of flow; especially in winter, the barotropic component may attain appreciable speeds (Schumacher and Reed, 1980, 1986).

Figure 30 shows the geopotential topography at 250 db referred to 150 db. Such a presentation is quite sensitive to the reference level chosen, and an actual level surface may vary in space and time. The results shown, however, appear plausible and are in agreement with the other evidence discussed that Shelikof Strait has an estuarine-like circulation. In March there was a fairly intense northward inflow throughout the system. In July and October, however, the inflow appeared to be considerably weaker than in winter. What might account for this difference? It seems that the most plausible mechanism may simply involve the depth of the mixed layer. As it

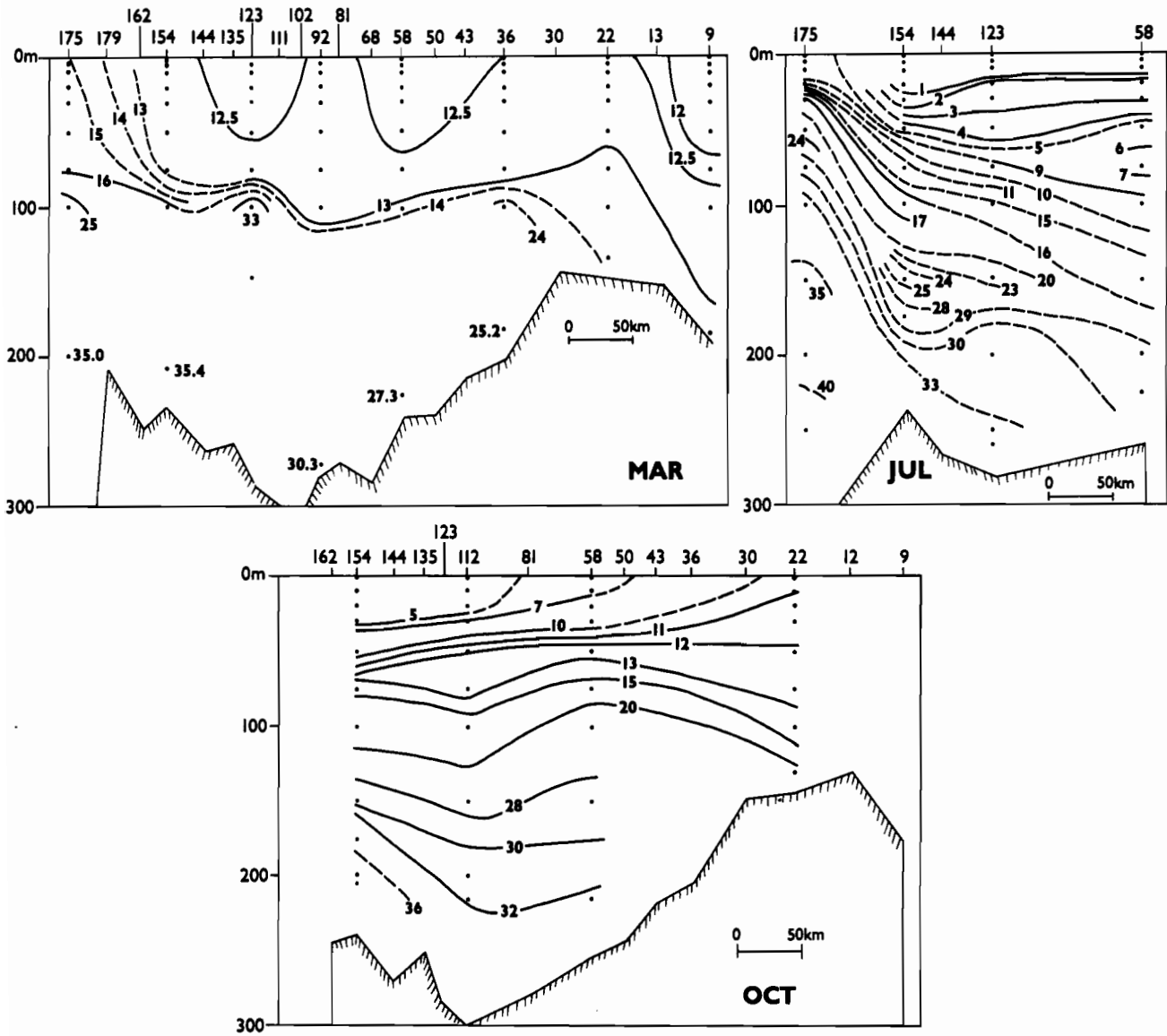


Figure 24.--Vertical sections of nitrate distribution (in $\mu\text{g-at}/\ell$) along the main channel in Shelikof Strait during March, July, and October 1985.

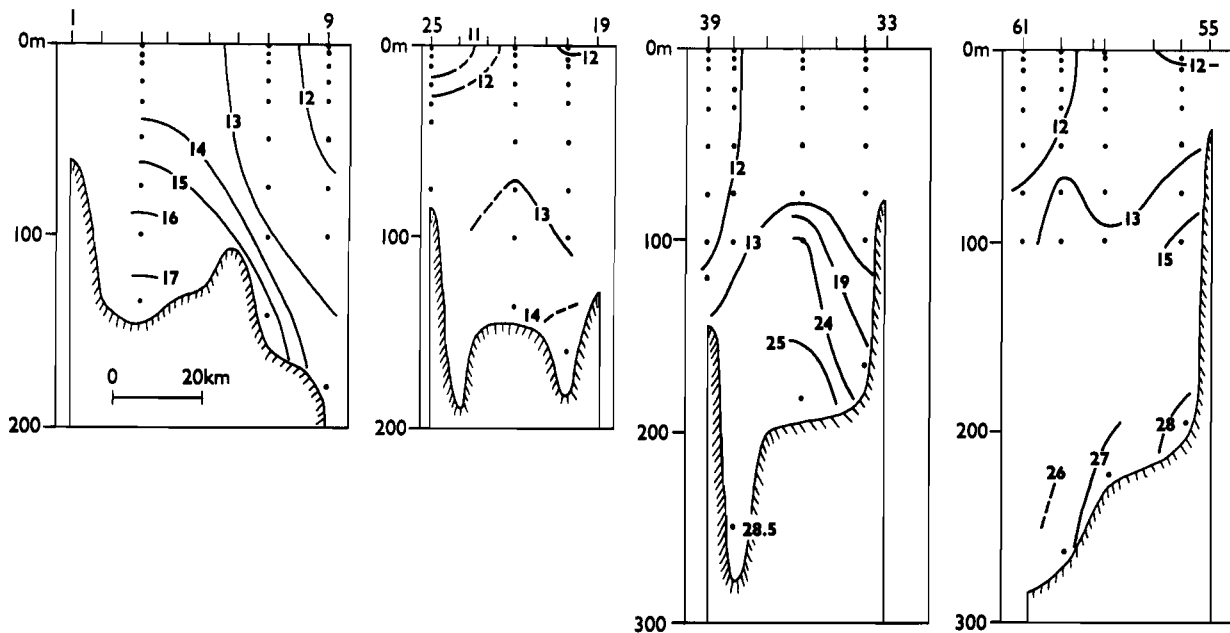


Figure 25.--Vertical sections of nitrate distribution (in $\mu\text{g-at/l}$) for stations 1-9, 19-25, 33-39, and 55-61, March 1985.

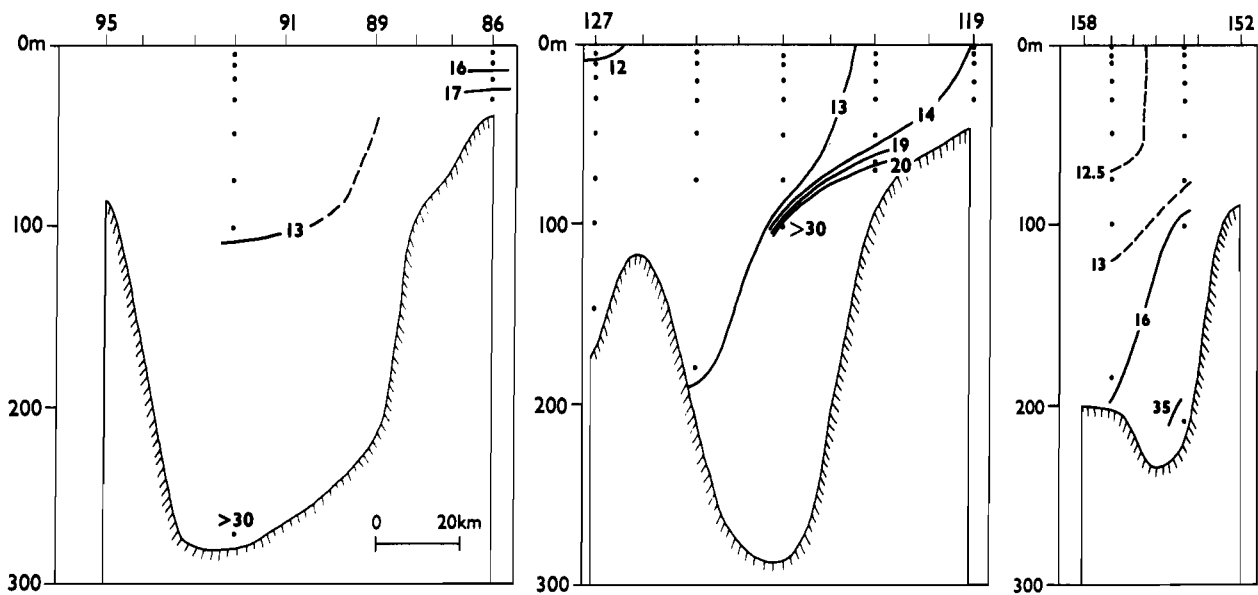


Figure 26.--Vertical sections of nitrate distribution (in $\mu\text{g-at/l}$) for stations 86-95, 119-127, and 152-158, March 1985.

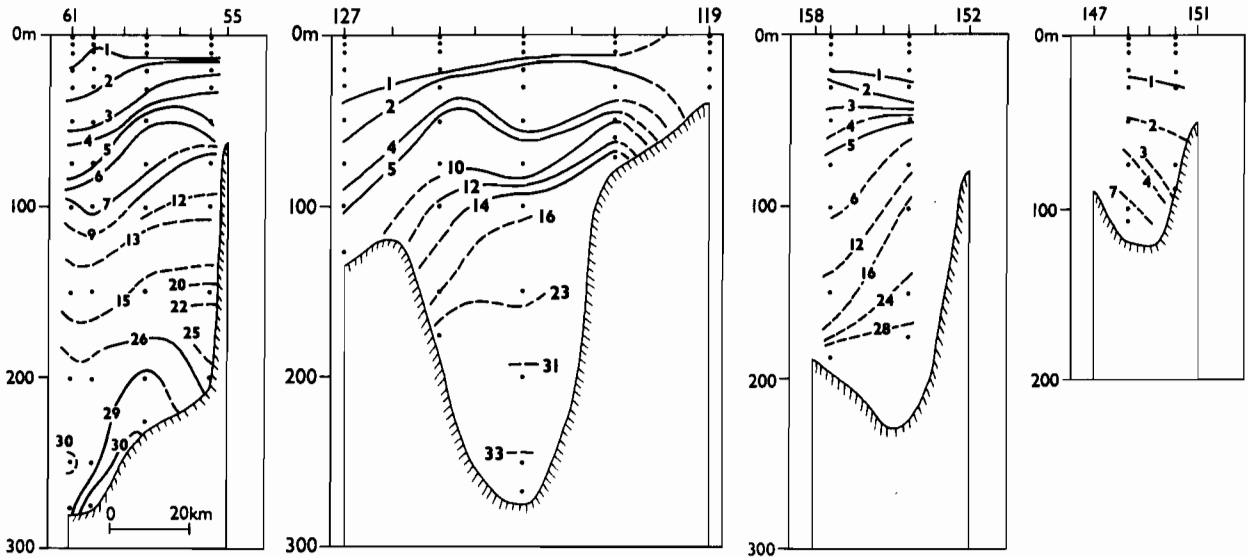


Figure 27.--Vertical sections of nitrate distribution (in $\mu\text{g-at}/\ell$) for stations 55-61, 119-127, 152-158, and 147-151, July 1985.

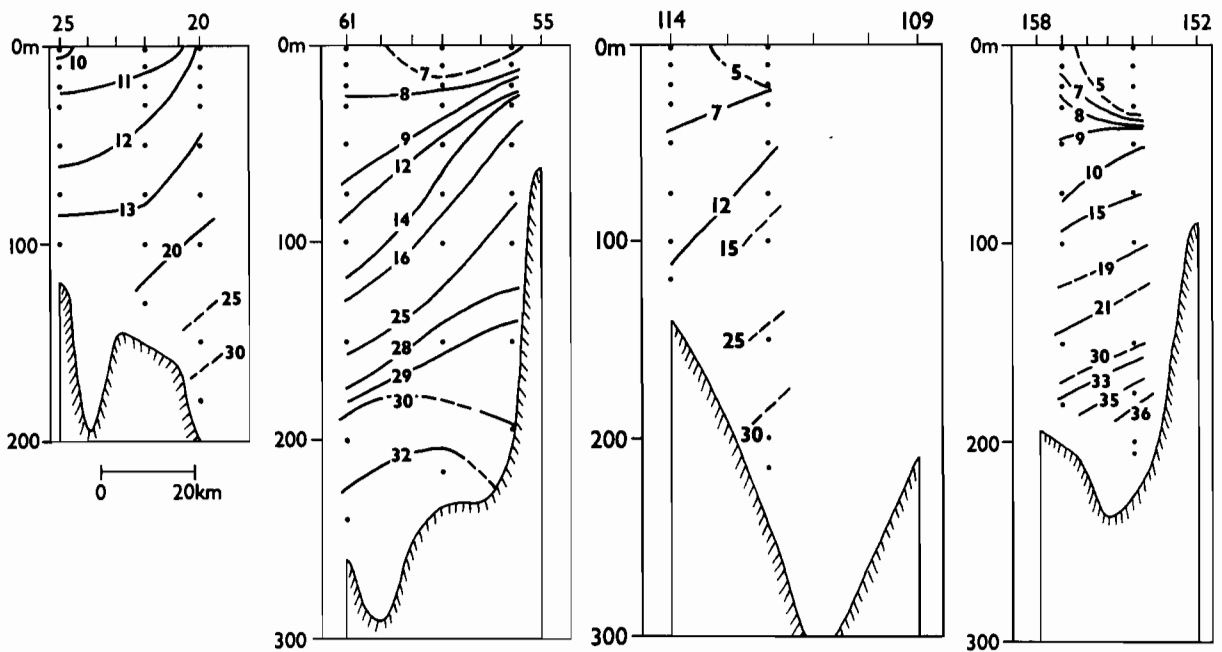


Figure 28.--Vertical sections of nitrate distribution (in $\mu\text{g-at}/\ell$) for stations 20-25, 55-61, 109-114, and 152-158, October 1985.

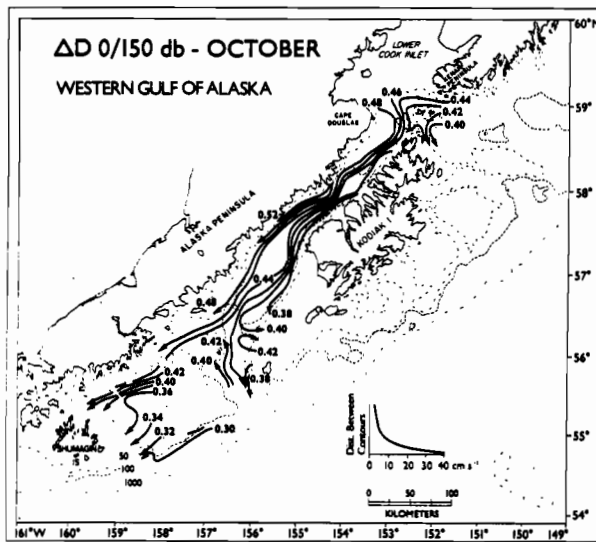
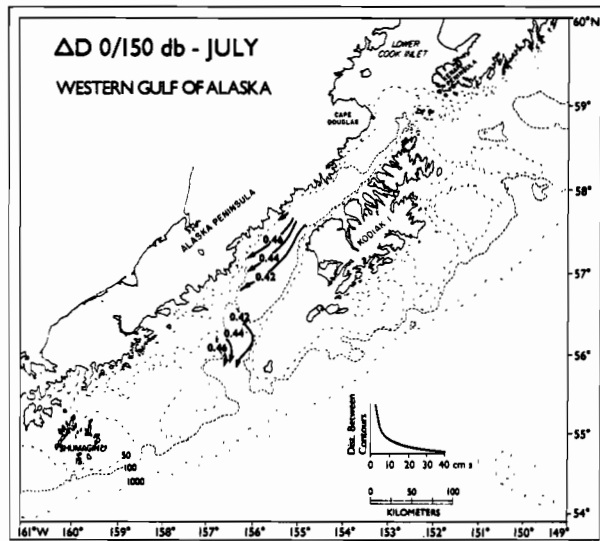
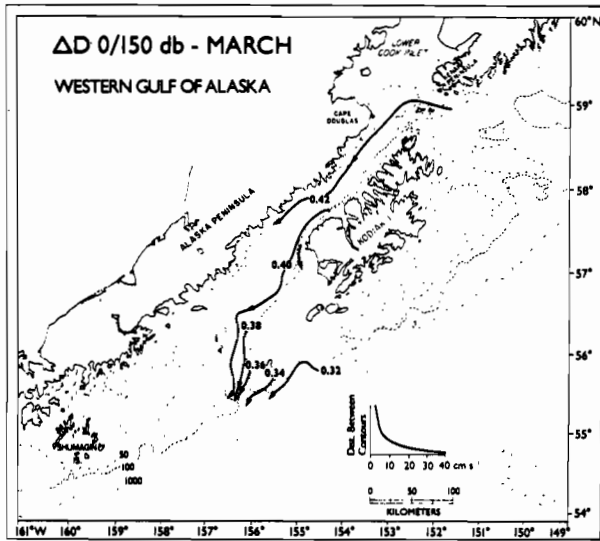


Figure 29.--Geopotential topography (ΔD , dyn m) of the sea surface, referred to 150 db, March, July, and October 1985.

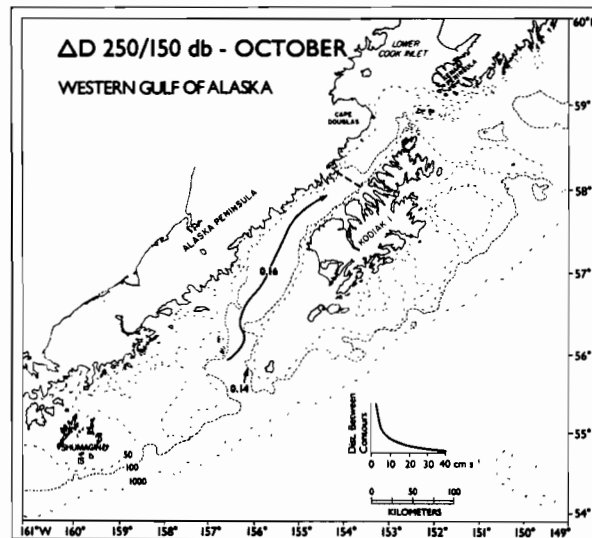
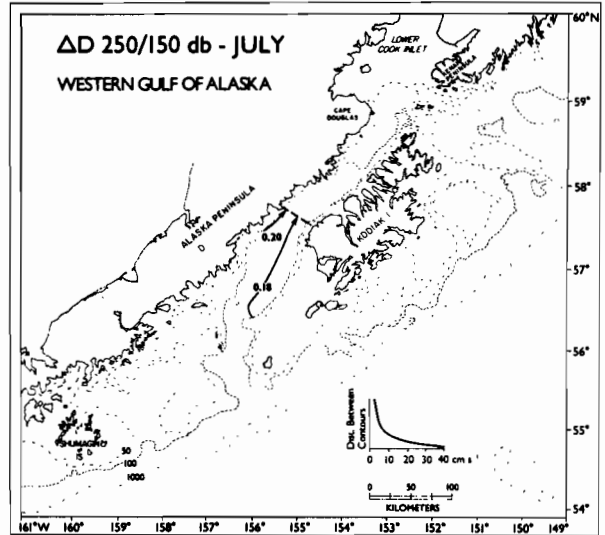
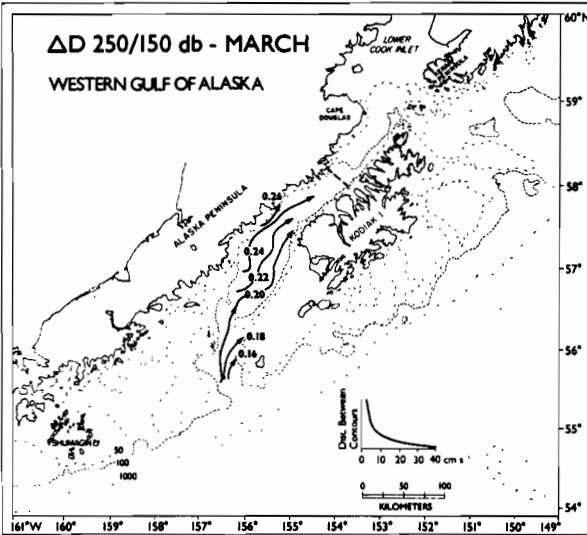


Figure 30.--Geopotential topography (ΔD , dyn m) of the 250-db surface, referred to 150 db, March, July, and October 1985. Dashed lines indicate the northern limit of data coverage.

deepens in winter through wind mixing, the cross-channel density gradients in deep water tend to be large (Figs. 9-12) and enhance the inflow. Also, March 1985 had much deeper mixed layers than limited data for winter 1978 and 1986 indicate (discussed below), and the inflow in winter 1985 was greater than at those times.

7. VOLUME TRANSPORT

Before examining the baroclinic volume transport estimates, we briefly discuss the possible magnitude of errors in these values. Aside from the fact that the reference level used may not be a level surface, there are errors associated with inaccuracies in the determination of temperature, salinity, and pressure. If we assume that the vertically integrated geopotential anomaly difference (over 150 db) may have an uncertainty of 0.5 dyn cm, a rough estimate of the transport error in the 150-db layer is $0.03 \times 10^6 \text{ m}^3 \text{ s}^{-1}$. Such errors between adjacent stations may combine to produce smaller or larger errors for an entire section; an occasional error of $0.1 \times 10^6 \text{ m}^3 \text{ s}^{-1}$ does not seem implausible, however. The effects of internal tides, if present, may contribute to even more uncertainty, especially in instances when some adjacent stations were not occupied sequentially. Thus some of the smaller differences shown below may not be real, but the larger features discussed are likely to be.

Table 3 presents volume transports, computed over 10-db intervals, for March. The 0 to 150-db transport entering Shelikof Strait (stations 1-9) was relatively small and remained so until stations 55-61. There was a further increase to $0.5 \times 10^6 \text{ m}^3 \text{ s}^{-1}$ on the next section downstream, then a rapid decrease, and fairly constant values thereafter, except for two of the more downstream sections which had values of $0.4 \times 10^6 \text{ m}^3 \text{ s}^{-1}$. Some possible reasons for this variability will be discussed below. All transports west of the sea valley were insignificant. Transports below 150 db also showed considerable variability, but there was a trend toward large deep-layer transport being associated with large upper-layer values. In fact the correlation coefficient between upper and deep estimates is 0.77, which is significant at the 99% level. Such a relationship does not hold for the other two cruises, however, nor is there any apparent relation between the absolute magnitudes of upper-layer and deep-layer transport throughout the year (see October data, Table 5). We suspect that the main factor affecting deep transport is mixed-layer depth as suggested above.

The July transport values are given in Table 4. Upper-layer values are comparable to those for March and again are fairly variable. A westward transport along the Alaska Peninsula (stations 147-151) was present in July, however. Deep transport in July over the same region of the Strait was considerably smaller than in March.

Table 5 presents the October transports. The upper transport in October, as expected, was the largest found. The variability was also quite large. The inflowing ACC had a value of $0.35 \times 10^6 \text{ m}^3 \text{ s}^{-1}$. (The southern part of the line bounded by stations 1-9 flowed eastward.) On the next line (stations 10-18) though the flow was eastward! Perhaps some of the ACC waters passed north of station 10. Beginning with the line between stations 26 and 32, transport exceeded the inflow, continued to increase, and reached a maximum of

Table 3.--Computed volume transport across CTD sections (with the bounding stations listed) for the upper 150 db and from 150 db to the bottom (using 150 db as the reference level), March 1985. The sections are arranged from north to south in the main channel of Shelikof Strait, with sections along the Alaska Peninsula listed last; positive values indicate westward or southward transport, and negative values indicate eastward or northward transport. Both positive and negative values are given for the line between stations 1 and 9.

Stations	Dates (March)	Volume transport ($10^6 \text{ m}^3 \text{ s}^{-1}$)			
		0 to 150 db	150 db to bottom	Total	
1-9	12-13	0.20	-0.05	0.00	0.15
10-18	13	0.07		0.00	0.07
19-25	13-14	0.10		---	0.10
26-31	14	0.17		0.00	0.17
33-39	14-15	0.17		-0.01	0.16
40-45	15	0.19		-0.04	0.15
46-53	15-16	0.19		-0.10	0.09
55-61	16	0.36		-0.18	0.18
62-70	16-18	0.53		-0.29	0.24
75-84	19	0.14		-0.13	0.01
88-95	19	0.18		-0.12	0.06
98-105	20	0.28		-0.17	0.11
108-114	20-21	0.23		-0.14	0.09
121-127	22	0.23		-0.11	0.12
132-140	22-23	0.23		-0.09	0.14
141-146	26	0.40		-0.18	0.22
152-158	25	0.30		-0.11	0.19
159-164	25	0.42		-0.21	0.21
177-184	24-25	0.27		-0.01	0.26
147-151	26	0.01		---	0.01
169-174	26-27	0.02		---	0.02
185-195	27	0.02		---	0.02

Table 4.--Same as Table 3 except for July 1985.

Stations	Dates (July)	Volume transport ($10^6 \text{ m}^3 \text{ s}^{-1}$)		
		0 to 150 db	150 db to bottom	Total
55-61	27-28	0.28	-0.09	0.19
121-127	27	0.46	-0.09	0.37
141-146	26	0.16	-0.02	0.14
152-158	25-26	0.43	-0.07	0.36
147-151	26	0.10	---	0.10

Table 5.--Same as Table 3 except for October 1985.

Stations	Dates (Oct)	Volume transport ($10^6 \text{ m}^3 \text{ s}^{-1}$)		
		0 to 150 db	150 db to bottom	Total
1-9	24-25	0.35	-0.22	0.13
10-18	25	-0.30	0.00	-0.30
20-25	25	0.22	---	0.22
26-32	22	0.50	0.00	0.50
33-39	22	0.59	-0.02	0.57
40-45	22	0.89	-0.04	0.85
46-53	21-22	0.71	-0.05	0.66
55-61	21	1.11	-0.03	1.08
78-84	21	0.10	-0.07	0.03
109-114	17-18	0.75	-0.06	0.69
120-127	17	0.57	-0.02	0.55
132-139	17	0.46	-0.01	0.45
141-146	10-11	0.20	-0.02	0.18
152-158	9	0.13	-0.03	0.10
159-164	13	0.09	-0.01	0.08
147-151	11	0.10	---	0.10
169-173	12	0.17	---	0.17
185-195	12	0.13	---	0.13
213-219	14	0.45	---	0.45
235-242	15	0.65	---	0.65
255-266	15-16	0.74	---	0.74
185-255	12-15	0.47	-0.01	0.46

$1.1 \times 10^6 \text{ m}^3 \text{ s}^{-1}$ at stations 55-61. The precipitous decrease on the next line downstream might be partially explained by this line not spanning the entire channel, but some decrease seems likely. The decrease on the last three sections in the main channel may have resulted from part of the flow being diverted westward; there is not a balance between the transport at stations 132-139 and the sum of those for stations 141-146 and 147-151, however. A striking feature in October is the small, generally insignificant deep-layer transport. Along the Alaska Peninsula west of about 158°W , there was a large increase in transport. This could be produced by a northward inflow into the region east of the Shumagin Islands. A computation of transport across the line bounded by stations 185 and 255 (see Fig. 2 and Table 5) does give a northward flow of $0.5 \times 10^6 \text{ m}^3 \text{ s}^{-1}$, which largely accounts for the increase found. Curiously, however, nearly all of this calculated inflow occurred between stations 185 and 208, and thus over the large bank there, rather than in the trough to the west.

What might produce so much variability in transport along the Shelikof sea valley? Some of the meandering seen in the geopotential topography may result from baroclinic instabilities in the flow and the propagation of waves downstream (Mysak et al., 1981). This seems unlikely to produce the large variations in transport, however. Some of the variation could result from our use of a constant reference level, whereas the true level surface may depart from this by varying amounts. Using the assumption that transport should remain relatively constant along the channel, we adjusted the reference level by varying amounts to yield approximate agreement with the inflow (stations 1-9). For March the maximum adjustment needed was only 40 m, but the October data frequently required moving the reference level up or down in excess of 75 m. Such large changes over short distances seem unlikely to us, and we find the computed variability more plausible than this for reasons discussed below.

A general feature common to both March and October was an abrupt increase in transport in the vicinity of Kodiak Island. This is a fairly constricted area with large orographic features on both the Alaska Peninsula and Kodiak Island. These features have effects on the wind field in their vicinity (Macklin et al., 1984), and a possible mechanism for producing changes in transport is differential Ekman pumping. We do not have continuous wind fields over large parts of the system, but shipboard observations indicated winds were frequently from the northeast. With these winds, and assuming a shear of 5 m s^{-1} between mid-channel and both mountainous coasts, a computation indicates that isopycnal slopes could be increased by 60 m in a week, which would increase volume transport. How such a spin-up would be translated downstream is hard to envision.

In addition to effects by winds, another mechanism also seems possible. This constricted region of the channel has a major change in depth. If significant barotropic flows are present, the downstream deepening could result in conversion of barotropic into baroclinic energy and thus an increase in transport computed by the geostrophic relation.

8. DISCUSSION

Spring 1985 was quite unusual in terms of the distribution of larval pollock. Ichthyoplankton sampling was conducted as a part of FOCI during mid-April and early May 1985. During April pollock eggs were found in greatest abundance below 150 m in the Strait, mostly northeast of the line from stations 55 to 61 and mostly over the deepest areas of the sea valley (A. Kendall et al., Northwest and Alaska Fisheries Center, unpublished data). This pattern agrees with the distribution of spawning pollock surveyed in late March 1985 (Nelson and Nunnallee, 1986; Fig. 3) and with the distribution of eggs sampled in April 1981 and 1982 (A. Kendall, unpublished data). Unlike other years sampled, however, larval pollock were extremely scarce in May 1985 (other surveys were conducted in May 1981, 1982, 1983, and 1986). The time between estimated hatching of eggs (mid-April) and the May 1985 larval survey (2-11 May) was very brief for biological processes to have accounted for the dramatic change in abundance. This suggests that the organisms, which live in the upper water column, had been very efficiently removed from the coastal environment by physical factors.

The line between stations 55 and 61 has been occupied 13 times between March 1978 and May 1986, and a comparison of the computed transports is given in Table 6. The two October upper-layer transports are similar, although deep transport in 1978 appears to have been much larger than in 1985. Comparison of the winter-spring transports indicates that 1985 had the greatest transports in both the upper and deep layers. Furthermore, the winter 1985 mixed layer was appreciably deeper than in winter 1978 or 1986. We suggested above that the depth of the mixed layer is an important constraint on the inflowing deep water; it would also strongly enhance the upper-layer flow when the deepest mixed layers occur on the right side of the Strait as was typical in winter 1985. Weather maps indicated unusual and persistently strong down-channel winds in March 1985, and the ocean seems to have responded in the manner expected. The vigorous circulation in winter-spring 1985 must have been a factor in removal of the larvae from the coastal region. Precisely how this occurred and the fate of the organisms remain unknown, however.

9. CONCLUSIONS

The following general conclusions about Shelikof Strait are supported by the data examined here. The deep and bottom water in Shelikof Strait has its source at the southern end of the Strait, and the properties of these waters vary considerably with time. The characteristics of the central and northern bottom waters appear to be attained through vertical mixing of the source waters in the southern part of the Strait. Thus Shelikof Strait seems to have an estuarine-type circulation with an upper layer flowing to the southwest and a deep layer flowing to the northeast. The intensity of the deep inflow varies greatly; maximum inflow seems to be linked to deep mixed layers which create large across-channel density gradients. The upper-layer outflow also varies appreciably in space and time, and it may be enhanced by deepening of the mixed layer, especially when this occurs preferentially on the right side of the channel looking downstream. Differential Ekman pumping might accomplish this if the down-channel winds have the expected shear. At any rate, winds appear to have important effects on the physical system and also seem to affect transport and mixing of planktonic communities, including the larvae of pollock spawning in Shelikof Strait.

Table 6.--Computed volume transport across the CTD section bounded by stations 55 and 61 for the upper 150 db and from 150 db to the bottom (using 150 db as the reference level) from 1978 to 1986. Positive values indicate southwest transport, and negative values indicate northeast transport.

Dates	Volume transport ($10^6 \text{ m}^3 \text{ s}^{-1}$)		
	0 to 150 db	150 db to bottom	Total
17 March 1978	0.22	-0.08	0.14
9 October 1978	0.80	-0.16	0.64
* 7 April 1981	0.04	-0.01	0.03
* 30 April 1981	0.11	---	?
* 22 May 1981	0.02	0.00	0.02
16 March 1985	0.36	-0.18	0.18
27-28 July 1985	0.28	-0.09	0.19
21 October 1985	1.11	-0.03	1.08
11 February 1986	0.26	-0.07	0.19
13 March 1986	0.27	-0.09	0.18
23 March 1986	0.28	-0.08	0.20
3 May 1986	0.17	-0.08	0.09
18 May 1986	0.26	-0.05	0.21

* These occupations did not completely span the channel.

10. ACKNOWLEDGMENTS

We thank the officers and crews of the NOAA ships DISCOVERER and MILLER FREEMAN. S. Froberg assisted in data processing, and K. Kroglund analyzed the nutrient samples. We appreciate conversations with A. Kendall and G. Stauffer of the Northwest and Alaska Fisheries Center and with R. Romea of the Pacific Marine Environmental Laboratory. This is a contribution to the Fishery-Oceanography Coordinated Investigations of NOAA.

11. REFERENCES

- Bretschneider, D.E., G.A. Cannon, J.R. Holbrook, and D.J. Pashinski (1985): Variability of subtidal current structure in a fjord estuary: Puget Sound, Washington, *J. Geophys. Res.*, 90, 11949-11958.
- Favorite, F., and W.J. Ingraham, Jr. (1977): On flow in northwestern Gulf of Alaska, May 1972, *J. Oceanogr. Soc. Japan*, 33, 67-81.
- Macklin, S.A., J.E. Overland, and J.P. Walker (1984): Low-level gap winds in Shelikof Strait, *Proc. Third Conference on Meteorology of the Coastal Zone*, American Meteorological Society, Boston, 97-102.
- Mysak, L.A., R.D. Muench, and J.D. Schumacher (1981): Baroclinic instability in a downstream channel: Shelikof Strait, Alaska, *J. Phys. Oceanogr.*, 11, 950-969.
- Nelson, M.O. and E.P. Nunnallee (1986): Results of acoustic midwater trawl surveys for walleye pollock in Shelikof Strait, 1985. Condition of groundfish resources of the Gulf of Alaska region assessed in 1985. NOAA Tech. Memo. NMFS-NWAF-106, 23-49.
- Reed, R.K., and J.D. Schumacher (1986): Physical oceanography of the Gulf of Alaska, *The Gulf of Alaska. Physical and Biological Environment*, D.W. Hood, ed. (in press).
- Royer, T.C. (1981): Baroclinic transport in the Gulf of Alaska, Part II. A fresh water driven coastal current, *J. Mar. Res.*, 39, 251-266.
- Schumacher, J.D., R. Sillcox, D. Dreves, and R.D. Muench (1978): Winter circulation and hydrography over the continental shelf of the northwest Gulf of Alaska, NOAA Tech. Rep. ERL 404-PMEL 31, 16 pp.
- Schumacher, J.D. and R.K. Reed (1980): Coastal flow in the northwest Gulf of Alaska: the Kenai Current, *J. Geophys. Res.*, 85, 6680-6688.
- Schumacher, J.D., L.S. Incze, S.A. Macklin, and A.W. Kendall, Jr. (1985): A fishery-oceanography experiment in the Gulf of Alaska. *Trans. Amer. Geophys. Union (EOS)*, 66, 1327.
- Schumacher, J.D., and R.K. Reed (1986): On the Alaska Coastal Current in the western Gulf of Alaska, *J. Geophys. Res.*, 91, 9655-9661.
- Whitledge, T., S. Malloy, C. Patton, and C. Wirick (1981): Automated nutrient analyses in seawater. BNL Rep. 51398, Brookhaven National Laboratory, Upton, N.Y., 216 pp.
- Xiong, Q., and T.C. Royer (1984): Coastal temperature and salinity in the northern Gulf of Alaska, 1970-1983, *J. Geophys. Res.*, 89, 8061-8068.